Polar Geosci., **13**, 1-40, 2000

Granulite-facies beryllium pegmatites in the Napier Complex in Khmara and Amundsen Bays, western Enderby Land, East Antarctica

Edward S. Grew[1], Martin G. Yates[1], Jacques Barbier[2], Charles K. Shearer[3], John W. Sheraton[4]*, Kazuyuki Shiraishi[5] and Yoichi Motoyoshi[5]

[1]*Department of Geological Sciences, University of Maine, 5790 Edward T. Bryand Global Sciences Center, Orono, Maine 04469-5790, U.S.A.*
[2]*Department of Chemistry, McMaster University, Hamilton, Ontario L8S 4M1, Canada*
[3]*Institute of Meteoritics, University of New Mexico, Albuquerque, New Mexico 87131, U.S.A.*
[4]*Department of Geology, Australian National University, Canberra 0200, A.C.T., Australia*
[5]*National Institute of Polar Research, Kaga 1-chome, Itabashi-ku, Tokyo 173-8515*

Abstract: Four granulite-facies beryllium pegmatites of Late Archean age intrude ultrahigh-temperature Napier Complex metapelites in Khmara Bay at "Christmas Point" and "Zircon Point" and in Amundsen Bay on Mt. Pardoe. The pegmatites evolved in three major stages. During the first stage, melt from anatexis of sapphirine-bearing metapelites soon after temperatures peaked during ultrahigh-temperature metamorphism crystallized as pegmatites in inter-boudin spaces during the waning stages of associated deformation. The primary carrier of beryllium in the pegmatites at the time of their intrusion was a sapphirine-group mineral. The second stage is high-temperature metamorphism at moderate pressure, which resulted in reaction of sapphirine with quartz to form corona assemblages of sillimanite+orthopyroxene (or garnet) in the host rocks and sillimanite+garnet+surinamite in the beryllium pegmatites. Previous investigators have attributed the corona assemblages to isobaric cooling following ultrahigh-temperature metamorphism, but the relatively large size of the coronas and their deformation in the pegmatites suggests that the coronas formed in both the host rocks and the pegmatites during a separate tectonothermal event. The third stage includes two metamorphic events at lower temperatures and moderate to low pressures when surimanite broke down to beryllian cordierite±Al-poor orthopyroxene. The presence of late-formed kyanite and andalusite in the pegmatites is consistent with decompression inferred by other investigators for these two events. Beryllium in the Late Archean pegmatites could have originated from the host granulites, which at "Christmas Point" and Mt. Pardoe have average Be contents of 3.8±2.4 ppm and 3.5±1.4 ppm, respectively. Beryllium content of host-rock sapphirine is 61 to 616 times whole-rock Be content, implying an important role for this mineral in supplying Be to the anatectic melt.

key words: pegmatite, beryllium, Antarctica, Archean/Archaean

*Present address: Stoneacre, Bream Road, St Briavels, Lydney, Glos GL15 6TL, U.K.

1. Introduction

Beryllium, a relatively rare element even in the upper continental crust (Taylor and McLennan, 1995; Wedepohl, 1995, calculated this abundance to be 3 ppm), has been reported in significant concentrations at five localities in the Napier Complex (Fig. 1). Beryllian sapphirine was found at Mt. Riiser-Larsen (Christy, 1989) and Gage Ridge (Grew, 1981), whereas pegmatites containing beryllium minerals have been described from three others. These pegmatites will be referred to as beryllium pegmatites in the present paper. Grew (1981) discovered one beryllium pegmatite each at "Christmas Point" in the Field Islands and "Zircon Point" (respectively, 5 km west-southwest and 2 km south of McIntyre Island) in Khmara Bay in December, 1979, while on the Australian National Antarctic Research Expedition (ANARE). In January, 1999, while on the 40th Japanese Antarctic Research Expedition (JARE-40), we were given the opportunity to revisit the discovery pegmatite at "Christmas Point" (67°23′S, 48°58′E GPS reading, 1984 world datum, C. Carson, personal communication), at which time a second beryllium pegmatite was found nearby. In addition, a beryllium pegmatite was discovered at 67°05′S, 51°40′E (GPS reading, 1984 world datum, C. Carson, personal communication), roughly 2 km southeast of the summit of Mt. Pardoe. The three beryllium pegmatites belong to the same generation, emplaced during the Late Archean at 2475±25 Ma, which also includes the "granulite-facies" and "sillimanite" pegmatites of other investigators (Grew *et al.*, 1982; Black *et al.*, 1983; Sandiford and Wilson, 1986; Grew, 1998). This generation is different from Early Palaeozoic pegmatites, some of which also contain Be minerals (*e.g.*, Grew, 1981).

Our understanding of the origin of the beryllium pegmatites has improved since the original report in 1981 (Grew, 1998). Critical relationships in samples obtained on JARE-40 confirm the origin first proposed by Franz and Morteani (1984) and De Roever and Vrâna (1985) and expanded by Grew (1998), according to which the beryllium

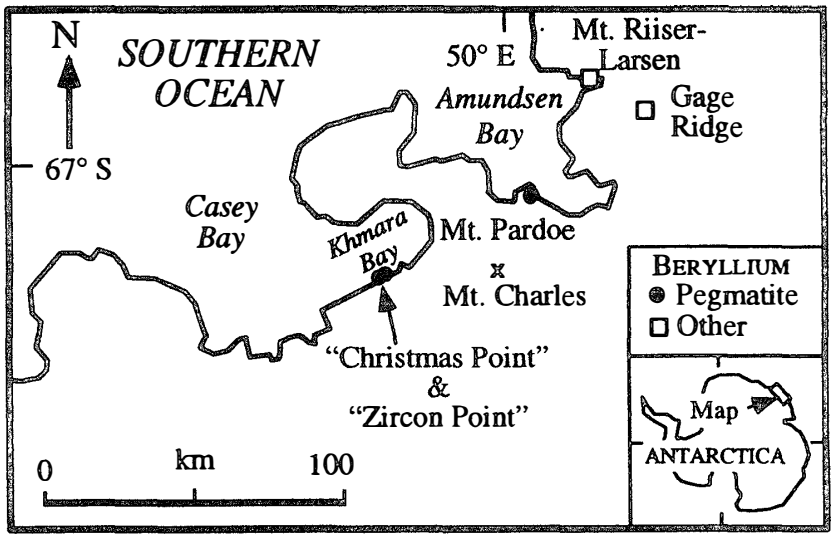

Fig. 1. Map of western Enderby Land showing location of beryllium pegmatites and of other beryllium enrichments not associated with pegmatites.

minerals surinamite, musgravite and chrysoberyl formed from the breakdown of a magmatic beryllium-bearing precursor during metamorphism following emplacement. In addition, the new samples provide convincing evidence that this precursor was a beryllian sapphirine-group mineral rather than beryllian cordierite, which Grew (1998) suggested although no evidence was preserved for an early formed cordierite.

The present paper reports petrographic and chemical data on samples from the three beryllium pegmatites studied on JARE-40 (including samples collected in 1979 on ANARE) and whole-rock chemistry on host rocks collected at "Christmas Point" on ANARE and at Mt. Pardoe on JARE-40. In addition, chemical data are presented on amphibole and pyroxene in a Late Archean pegmatite from Mt. Charles, nearly 30 km south of Mt. Pardoe (Fig. 1). Because U-Pb data indicate that the beryllian pegmatites and Mt. Charles pegmatite are coeval (Grew and Manton, 1979; Grew *et al*., 1982; Grew, 1998), their histories should be comparable.

Numbers for samples collected on ANARE begin 22. . . , *e.g*., 2234 L, 2292 C, whereas numbers for samples collected on JARE-40 begin with EG9901. . . and have been shortened to 1. . . , *e.g*., EG99012262 is referred to as 12262.

2. Host rocks and field relations

2.1. "Christmas Point"

The beryllium pegmatites at "Christmas Point" (Fig. 2a) are hosted by a subvertical layer of quartz-rich granulites about 15 m thick and extending roughly 100 m S 70°E. About 6 or 8 *en echelon* pods of pegmatite are present over the extent of the layer; they trend N55° to 60°E, dip 70° to 85°S and are deformed. The granulite layer is bounded on the north by garnet gneiss and on the south by a shear zone. Black *et al*. (1983, Fig. 2b) mapped this part of "Christmas Point" as pink gneiss as opposed to gray gneiss, which was interpreted by these authors to result from retrogressive metamorphism of the pink gneiss. While studying the area in 1979, the senior author found that the gneisses surrounding the granulite layer were both pink and gray, although the granulites and beryllium pegmatites sampled for the present study were from an area contiguous to the pink gneiss and were relatively little affected by this retrogression.

The layer is composed dominantly of indistinctly layered quartz-rich granulites (Table 1) in which a 15-cm-thick lens of two-pyroxene-garnet granulite is present. The most abundant type of quartz-rich granulite contains subordinate feldspar. Sillimanite, orthopyroxene, zircon and rutile are present in all the studied samples; garnet, sapphirine and monazite are present in most. Secondary biotite (after orthopyroxene ?) is nearly ubiquitous, whereas secondary cordierite (after garnet ?) was only found sparingly in one section. Sapphirine is rarely in direct contact with quartz (Fig. 3a); more commonly, it is overgrown by sillimanite aggregates or prisms. Sillimanite in turn is overgrown by orthopyroxene (Fig. 3b) or garnet (Figs. 3b, 3c). Platelets of corundum occur in the sillimanite coronas adjacent to sapphirine or are clustered in the center of a sillimanite aggregate, indicating the former presence of sapphirine. Orthopyroxene also forms grains up to 3.5 mm across. The textures in these granulites suggests that two generations of orthopyroxene and garnet are present; the original assemblage could have been Qtz+Spr+Opx$\pm$ Grt$\pm$Kfs; sapphirine reacted subsequently with quartz to form corona assemblages Opx+

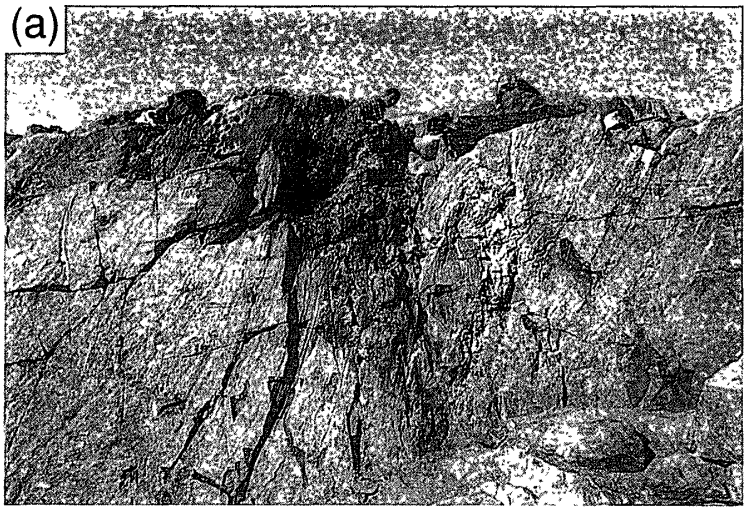

Fig. 2. Photographs of the beryllium and associated pegmatites.

(a) View roughly southeast of discovery pegmatite (red) in gray quartz granulite at "Christmas Point". Compositional layering in granulite is deformed in vicinity of pegmatite, which itself is broken up. Photograph is courtesy of Dan Dunkley.

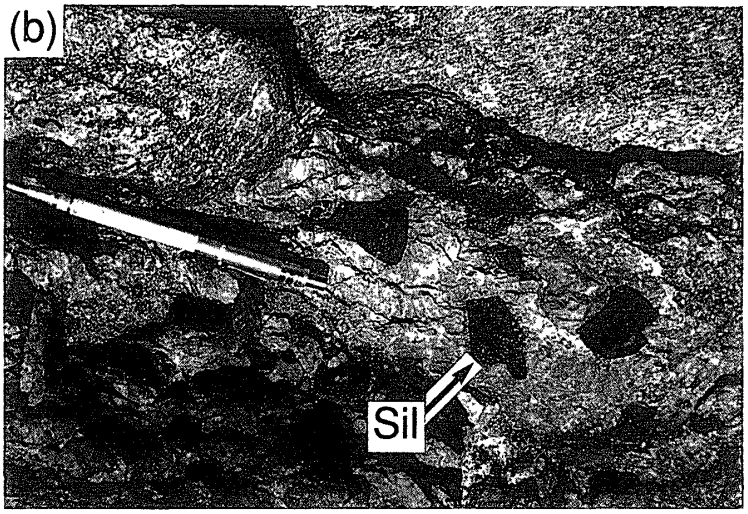

(b) Close up of a fragment of the discovery pegmatite with centimeter-sized brown sillimanite prisms (Sil). Photograph is courtesy of Dan Dunkley.

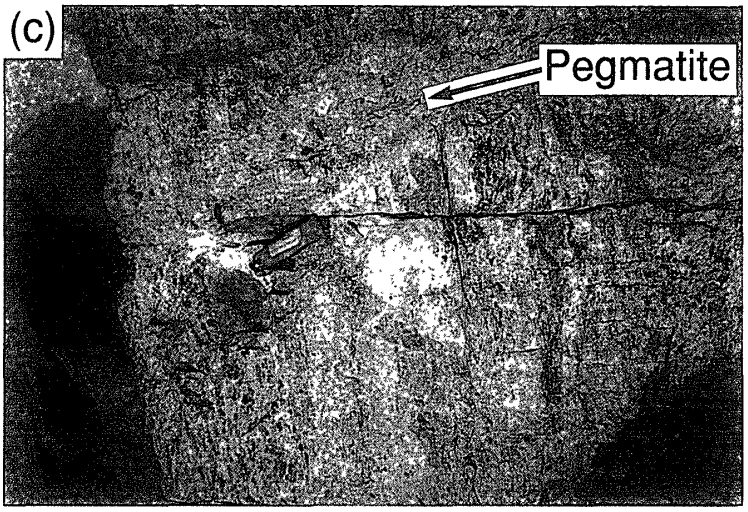

(c) Block of quartz granulite and crosscutting pegmatite, one of the three sampled, but not surinamite-bearing, at Mt. Pardoe.

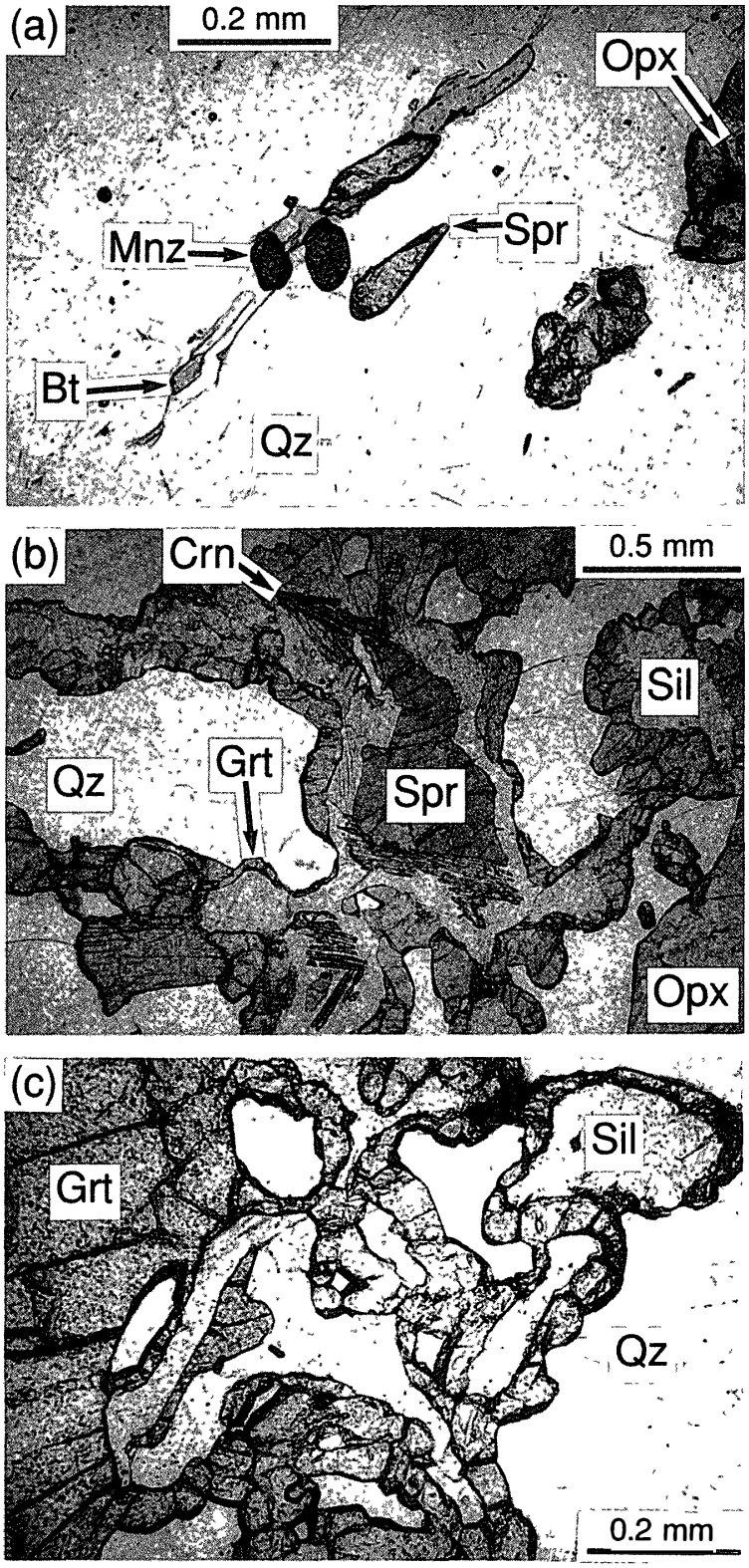

Fig 3 Photomicrographs of quartz granulites from "Christmas Point" Plane light

(a) Sapphirine (Spr) in direct contact with quartz near monazite (Mnz) (Sample 2292M)

(b) Sapphirine surrounded by inner corona of sillimanite (Sil) containing bundles of corundum platelets (Crn) and an outer corona dominated by orthopyroxene (Opx), garnet (Grt) appears locally (Sample 2292J)

(c) Sapphirine (blue) surrounded by inner corona of sillimanite and an outer corona of garnet, coarse garnet presumed to be coeval with sapphirine (Sample 2292J)

Table 1 Minerals of the pegmatites and host rocks and the abbreviations for mineral names used throughout this paper

Locality		"Christmas Point"			"Zircon Point"[1]	Mt Pardoe	
Rock type, pegmatite number		N° 1	N° 2	QG[2]	Peg	Peg[3]	QG[2]
Number of samples		19	15	9	4	8	9
Quartz (Qtz, Qz)		X	X	X	X	X	X
Alkali feldspar (Kfs)	Intergrowths, mesoperthite (Fsp)	X	X	X	X	X	X / X
Plagioclase (Pl)		T	T	T	T		X
Sillimanite, coarse (Sil)		X	X	X	–	–	–
Sillimanite, medium- or fine-grained (Sil)		X	X	X	X	X	X
Kyanite (Ky)		T	T	–	T	T	–
Andalusite (And)		T	–	–	–	T	–
Orthopyroxene, coarse (Opx)		–	–	–	–	X	–
Orthopyroxene, medium- or fine-grained		T	T	X	–	T	X
Orthoamphibole (Oam)		T	–	T	–	–	–
Clinoamphibole (Cam)		–	–	T	–	–	–
Garnet (Grt)		X	X	X	X	X	X
Biotite, coarse (Bt)		X	X	–	–	–	–
Biotite, fine (Bt)		X	X	X	X	X	X
Muscovite (Ms)		T	T	T	–	T	–
Chlorite (Chl)		T	T	T	–	–	–
Cordierite (Crd)		X	T	T	–	X	T
Sapphirine-khmaralite, coarse (**Spr, Khm**)		–	X	X	X	–	T
Sapphirine included in K-feldspar (**Spr**)		T	T	–	–	–	–
Surinamite (Sur)		X	X	–	X	T	–
Dumortierite (Dum)		–	–	–	T	–	–
Zircon (Zrn)		T	T	X	–	T	X
Apatite (Ap)		X	X	–	X	X	–
Wagnerite (Wag)		X	X	–	–	X	–
Monazite (Mnz)		X	T	X	T	X	X[4]
Xenotime (Xnt)		T	–	–	–	–	–
Corundum (Crn)		T	X	X	–	–	–
Ilmenite-hematite intergrowths (Ilm-Hem)		X	X	–	–	–	–
Magnetite (Mgt)		X	T	–	–	–	–
Spinel (Spl)		T	T	–	T	T	–
Hogbomite (Hog)±nigerite (?)		T	–	–	–	–	–
Musgravite (Mgr)		–	X	–	X	–	–
Chrysoberyl (Cb)		–	–	–	X	–	–
Rutile (Rt)		T	X	X	X	X	X
Sulfide		T[5]	T	–	–	T	–

Note Bold—mineral containing essential beryllium or potentially incorporating significant amounts X—Present in most samples or abundant in a few T—Present in relatively few sections and never abundant Selection of mineral abbreviations is based on list in Appendix of booklet "The Nomenclature of Minerals A Compilation of IMA Reports" published in 1998 by the Mineralogical Association of Canada, which is derived largely from Kretz (1983) [1]From Grew (1981) and Barbier *et al* (1999) [2]Quartz-rich granulite host rocks [3]From three pegmatite veins [4]In one section, Th dominant (huttonite ?) [5]Sulfide is pyrite in one case

Sil and Grt+Sil. Corundum formed in isolation from quartz from sapphirine breakdown. Biotite and cordierite apparently formed during a later event Sandiford (1985a) reported similar textures in metapelites from the Fyfe Hills.

Another type of quartz-rich granulite contains conspicuous garnet Sillimanite is present in quartz segregations as abundant, brown prisms up to 2 cm across and over 7 cm long that resemble the very coarse sillimanite prisms found in the beryllium pegmatites In one section, orthoamphibole and rare clinoamphibole formed with cordierite from garnet breakdown, in textures similar to those described by Sandiford (1985b) and Harley (1985b).

2.2. Mt. Pardoe

The pegmatites and their quartz granulite hosts (Fig 2c) were found in loose blocks that most likely formed by break up of outcrop without further transport Nodules up to several centimeters across in the granulites are rich in orthopyroxene and sillimanite, sapphirine occurs locally (Table 1). Both sillimanite and orthopyroxene are present in two generations. Early formed sillimanite forms kinked prisms 0 2–1.5 mm across and up to nearly 4 mm long; early orthopyroxene grains 1–8 mm across are characterized by fine, oriented rutile needles. Later formed sillimanite forms fringes on sillimanite prisms and fine-grained aggregates with orthopyroxene . Two generations of garnet, which is less abundant, are also present: (1) medium-sized grains, and (2) aggregates of small grains, in part symplectitic with quartz, and typically found around early garnet, between sillimanite and orthopyroxene, or between orthopyroxene grains Sapphirine forms localized patches of small, clustered grains, rarely exceeding 1 mm across, in sillimanite; in places, sapphirine is separated from quartz by a sillimanite selvage 0 02–0 03 mm thick Cordierite occurs in the sillimanite-orthopyroxene aggregates in a few sections Streaking out of sillimanite-orthopyroxene aggregates, granulation of feldspar and suturing of quartz-grain boundaries are all indicative of partial cataclasis of the granulites, which has resulted in a flinty appearance in some specimens

3. Bulk analyses of the host rocks

At "Christmas Point" seven of the eight analyzed samples (no 2292F-M) of the quartz-rich granulite were collected over a distance of 5 m across strike in the vicinity of the discovery pegmatite The eighth (no 2282G) was collected from the same layer, but ~100 m distant and not near a known beryllium pegmatite At Mt Pardoe, the four analyzed samples (different layers of no 10502 were analyzed individually) were collected from loose blocks of local origin over the area not exceeding 10 m^2 where the studied pegmatites were sampled.

The rocks were analyzed by the following methods at the Australian National University (ANU) (1) X-ray fluorescence (XRF) using glass discs - Si, Ti, Al, total Fe, Mn, Mg, Ca, Na, K, P, S, Cl, (2) XRF using pressed powders - Y, Zr, Nb, Cs, Hf, Ta, La, Ce, Pr, Nd, Th, U, Sc, V, Ni, Cu, Zn, Ga, Ge, As, Se, Br, Nb, Mo, Ag, Cd, In, Sn, Sb, Te, I, Tl, Pb, Bi, Cr, Rb, Sr, Ba CO_2, $H_2O(-)$ and $H_2O(+)$ were done at ANU using a Leco combustion furnace under a N_2 atmosphere $H_2O(-)$ was measured at 120°C, $H_2O(+)$ and CO_2 at 1040°C Fe^{2+} was determined by dichromate titration after dissolving the sample in acid The remaining elements were measured at Analabs, Welshpool, Western

Table 2 Whole rock analyses of quartz-rich granulites from "Christmas Point"

Sample No	2282G	2292F	2292G	2292H	2292J	2292K	2292L	2292M	Average	Std dev
					wt%					
SiO_2	77 65	79 03	74 75	79 24	74 72	78 93	78 37	79 19	77 73	1 9
TiO_2	0 61	0 63	0 82	0 58	1 10	0 60	0 61	0 55	0 69	0 2
Al_2O_3	13 80	11 22	12 01	10 46	9 24	9 80	10 45	11 90	11 11	1 5
Fe_2O_3	0 78	1 27	1 28	1 09	2 51	1 38	0 93	0 59	1 23	0 6
FeO	1 35	2 64	2 24	2 28	3 48	2 90	2 04	1 31	2 28	0 7
MnO	0 006	0 013	0 012	0 015	0 028	0 012	0 010	0 006	0 013	0 0
MgO	3 63	4 00	6 56	4 50	8 41	4 41	5 25	5 03	5 22	1 6
CaO	0 24	0 18	0 07	0 19	0 12	0 18	0 09	0 02	0 13	0 1
Na_2O	0 21	0 08	0 11	0 28	0 03	0 15	0 23	0 04	0 14	0 1
K_2O	0 54	0 27	0 80	0 71	0 06	0 81	0 89	0 73	0 60	0 3
S	0 013	0 010	0 014	0 015	0 024	0 014	0 012	0 018	0 015	0 0
P_2O_5	0 190	0 049	0 036	0 014	0 018	0 036	0 027	0 064	0 054	0 1
F	0 03	0 00	0 12	0 01	0 00	0 01	0 08	0 08	0 04	0 0
O=F, Cl	-0 02	0 00	-0 05	-0 01	0 00	0 00	-0 03	-0 04	-0 02	
Total	99 48	99 62	99 02	99 63	99 94	99 48	99 21	99 77	99 52	
					ppm					
Li	4 0	6 2	21 3	10 4	11 1	5 4	12 9	4 3	9 5	5 8
Be	7 1	1 4	5 5	2 7	3 1	0 8	2 5	6 9	3 8	2 4
B	<20	<20	<20	<20	<20	<20	<20	<20	—	
F	305	<50	1150	105	<50	55	805	830	406	455
Cl	317	88	21	120	43	16	34	36	84	100
Sc	6	14	22	20	34	14	20	12	18	8
V	8	10	30	22	38	8	14	8	17	12
Cr	<2	2	12	2	16	2	<2	<2	4 3	6
Ni	<1	<1	4	<1	<1	<1	<1	<1	—	
Cu	15	<1	<1	<1	<1	<1	<1	<1	—	
Zn	11	8	15	12	21	10	14	11	13	4
Ga	22	16	24	17	17	18	20	21	19	2 7
Ge	<0 9	<1	<0 7	<0 9	<0 9	<0 9	<0 8	<0 8	—	
As	<0 4	<0 3	0 4	0 3	<0 3	<0 3	0 3	<0 3	—	
Se	<0 4	<0 4	<0 3	<0 4	<0 4	<0 4	<0 3	<0 4	—	
Br	1 9	1 3	0 5	1 6	1 1	1 4	0 7	0 5	1 1	0 5
Rb	12	3	18	9	1	11	12	14	10	6
Sr	5	3	4	12	1	9	6	2	5 3	4
Y	346	121	101	180	230	86	133	142	167	85
Zr	481	673	754	722	817	697	736	548	678	111
Nb	22	28	38	28	55	23	30	32	32	10
Mo	0 5	<0 5	<0 5	<0 5	<0 6	0 5	<0 5	<0 5	—	
Ag	0 1	<0 1	<0 1	<0 1	<0 1	<0 1	<0 1	<0 1	—	
Cd	<0 1	<0 1	<0 1	0 1	<0 1	0 1	<0 1	<0 1	—	
In	<0 1	<0 1	<0 1	<0 1	<0 1	<0 1	<0 1	<0 1	—	
Sn	6 9	2 3	4	2 3	4 4	2 9	3 6	3 7	3 8	1 5
Sb	0 3	<0 1	<0 1	<0 1	0 2	<0 1	0 1	<0 1	0 1	0 1
Te	<0 2	<0 2	<0 2	<0 2	<0 2	<0 2	<0 2	<0 2	—	
I	<0 4	<0 4	<0 4	<0 4	<0 3	<0 4	<0 4	<0 4	—	
Cs	<0 6	<0 5	<0 5	<0 5	<0 4	<0 5	<0 5	<0 5	—	

Table 2 Continued

Sample No	2282G	2292F	2292G	2292H	2292J	2292K	2292L	2292M	Average	Std dev
					ppm					
Ba	345	247	541	774	36	831	624	409	476	270
La	453	164	103	33	42	98	71	212	147	138
Ce	916	342	210	51	87	193	141	435	297	281
Pr	125	37	20	2	2	18	10	56	34	41
Nd	315	125	70	15	30	70	45	140	101	97
Hf	17	21	22	21	24	21	23	15	20	3
Ta	4	6	3	5	7	2	4	4	4 4	1
Tl	1 6	1 6	0 4	1 1	0 6	1 3	0 6	0 8	1 0	0 5
Pb	36	12	10	4	4	10	7	16	12	10
Bi	1 2	1 2	0 6	0 5	0 6	1	0 6	0 8	0 8	0 3
Th	265	99	57	13	23	56	40	113	83	81
U	19	4	6	2	4	4	4	9	6 5	5 5
					Selected critical element ratios					
mg	0 76	0 65	0 77	0 71	0 72	0 65	0 77	0 83	0 73	0 1
k	0 62	0 69	0 82	0 62	0 54	0 78	0 72	0 92	0 71	0 1
ASI	10 08	15 26	10 27	6 63	28 12	6 83	6 90	13 27	12 17	7 2
K/Rb	359	667	370	649	507	608	639	432	529	129
K/Pb	123	182	662	1373	127	689	1030	383	571	457
Be/Nd	0 023	0 011	0 079	0 180	0 103	0 011	0 056	0 049	0 06	0 1

Note Std Dev = standard deviation < indicates element is below detection with the number being the detection limit Ratios mg = Mg/(Mg + total Fe), k = K/(K + Na), ASI = Al/(K + Na + 2Ca), all molecular

Australia as follows. (1) inductively coupled plasma mass spectrometry (ICP-MS)—Li, Be, (2) inductively coupled plasma atomic emission spectrometry (ICP-AES)—B, and (3) ion sensitive electrode—F

The beryllium contents of the quartz-rich granulites from "Christmas Point" average 3 8 $\pm$ 2.4 ppm Be (Table 2) and from Mt Pardoe, 3.5 $\pm$ 1.4 ppm Be (Table 3; the SiO_2-rich sample 10502a is excluded from the average because dilution of other constituents skews the average), comparable to the average of 3.7 $\pm$ 4 7 ppm Be for 25 Napier complex metapelites from south and east of Amundsen Bay (Sheraton, 1980, 1985, unpublished data). Overall, compositions of granulites from both localities are similar to those of the Cr-poor Napier metapelites of Sheraton (1980). they have low V, Cr and Ni contents and high SiO_2 contents, *i.e*, they are metapsammo-pelites The high SiO_2 contents only partly accounts for their lower V, Cr and Ni contents. The Cr-poor metapelites and quartz granulites are unusually magnesian, *i.e*, they have high mg numbers and MgO contents In addition, the "Christmas Point" quartz-rich granulites are unusually enriched in Y, La, Ce, Th, and U compared to the Mt Pardoe granulites, other Napier Complex metapelites, and granulite-facies metapelites from Prydz Bay (Sheraton *et al*, 1984).

Table 3 Whole rock analyses of quartz-rich granulites from Mt Pardoe

Sample No	10501	10502a	10502b	10505	10513	Average	Std dev
			wt%				
SiO_2	71 28	94 18	70 91	71 44	79 64	73 32	4 2
TiO_2	0 23	0 13	0 13	0 21	0 14	0 18	0 0
Al_2O_3	15 13	2 94	16 11	15 34	9 44	14 00	3 1
Fe_2O_3	1 58	0 21	0 80	1 59	0 76	1 18	0 5
FeO	2 58	0 54	2 42	2 14	2 03	2 29	0 3
MnO	0 054	0 010	0 042	0 045	0 030	0 043	0 0
MgO	7 23	1 43	6 49	6 84	4 43	6 25	1 2
CaO	0 12	0 08	0 40	0 26	0 48	0 31	0 2
Na_2O	0 43	0 31	1 31	1 01	1 30	1 01	0 4
K_2O	0 93	0 32	1 27	1 26	1 31	1 19	0 2
S	0 005	0 004	0 007	0 005	0 004	0 005	0 0
P_2O_5	0 007	0 005	0 013	0 009	0 009	0 010	0 0
F	0 01	0 02	0 02	0 01	0 02	0 02	0 0
O=F, Cl	0 00	-0 01	-0 01	-0 01	-0 01	-0 01	
Total	99 67	100 20	100 04	100 27	99 69	99 92	
			ppm				
Li	7 9	6 0	7 6	6 8	8 2	7 6	0 6
Be	3 7	0 7	2 7	2 3	5 4	3 5	1 4
B	<20	<20	<20	<20	<20	—	
F	110	180	240	90	160	150	67
Cl	15	15	20	63	<10	25	27
Sc	8	<2	6	6	6	7	1
V	14	4	8	10	12	11	3
Cr	4	<2	2	4	2	3	1
Ni	10	4	14	12	12	12	2
Cu	4	<2	4	4	4	4	0
Zn	82	19	73	79	78	78	4
Ga	28	5	25	26	26	26	1
Ge	<0 7	<0 8	<0 7	<0 6	<0 6	—	
As	<0 2	0 4	<0 2	<0 2	<0 2	—	
Se	<0 3	<0 4	<0 3	<0 3	<0 3	—	
Br	<0 2	1 0	0 8	0 2	0 2	0 3	0 3
Rb	20	3	10	10	10	12	5
Sr	6	3	23	15	15	15	7
Y	75	12	33	38	37	46	19
Zr	264	33	214	221	228	232	22
Nb	5	<1	<1	3	3	3	2
Mo	0 3	0 8	0 6	1 2	1 2	0 8	0 5
Ag	<0 1	0 1	0 1	<0 1	<0 1	—	
Cd	<0 1	0 2	0 1	<0 1	0 1	—	
In	<0 1	<0 1	<0 1	<0 1	<0 1	—	
Sn	0 8	0 6	0 9	0 8	0 6	0 8	0 1
Sb	<0 1	0 3	0 1	0 1	<0 1	—	
Te	<0 2	<0 2	<0 2	<0 2	<0 2	—	
I	<0 3	<0 3	<0 4	<0 4	<0 4	—	
Cs	<0 4	0 3	<0 5	<0 5	<0 5	—	
Ba	131	47	279	229	219	215	62

Table 3 Continued

Sample No	10501	10502a	10502b	10505	10513	Average	Std dev
			ppm				
La	17	15	92	61	57	57	30
Ce	34	34	158	107	106	101	51
Pr	2	3	17	8	4	8	7
Nd	9	9	48	31	24	28	16
Hf	12	3	9	9	9	10	1
Ta	2	<1	2	2	3	2	0
Tl	0 6	0 8	0 3	0 3	0 3	0 4	0 2
Pb	6	7	10	8	8	8	1
Bi	<0 2	0 6	0 3	<0 2	<0 2	—	
Th	23	48	38	31	30	30	6
U	1	1	2	1	2	1 6	0 4
			Selected critical element ratios				
mg	0 76	0 78	0 79	0 77	0 74	0 77	0 02
k	0 59	0 41	0 39	0 45	0 40	0 46	0 09
ASI	7 86	2 93	3 79	4 38	2 13	4 54	2 41
K/Rb	385	987	1065	1091	1143	921	359
K/Pb	1209	386	1098	1247	1374	1232	114
Be/Nd	0 430	0 079	0 056	0 075	0 225	0 197	0 2

Note Average is computed for four samples only, the SiO_2-rich sample 10502a is excluded Std Dev — standard deviation < indicates element is below detection with the number being the detection limit Ratios mg=Mg/(Mg+total Fe), k=K/(K+Na), ASI=Al/(K+Na+2Ca), all molecular

4. The beryllium pegmatites

4.1. "Christmas Point"

Of the four pegmatites at the "Christmas Point" locality studied on JARE-40, only two, the discovery pegmatite (no 1, Table 1) and one other (no 2) contain beryllium minerals, cordierite and wagnerite

Characteristic of the two beryllium pegmatites are prisms of brown sillimanite up to 10 cm long and 4 cm across (Fig 2b), masses of orange wagnerite up to nearly 5 cm across (*e.g*, Fig 4a) and yellow-brown apatite, red microcline, gray quartz, biotite in flakes several centimeters across or in medium-grained aggregates, and surinamite-bearing aggregates up to several centimeters across Both pegmatites have a quartz core, where the surinamite-bearing aggregates are more abundant, and an outer zone rich in microcline The surinamite aggregates are estimated to constitute roughly 5% of the quartz core in the discovery pegmatite, but <1% of the pegmatite as a whole Nodules up to 5 cm across of coarse-grained sapphirine-khmaralite in quartz are unique to the second beryllium pegmatite (Fig 4b)

Microcline commonly forms medium-grained lenticular aggregates, which give microcline-quartz portions of the pegmatite a sheared appearance In thin section, microcline is clouded with reddish particles (hematite ?) Microcline in both beryllium pegmatites locally contains fine (typically 0 02–0 1 mm) inclusions of sapphirine (Fig 5)

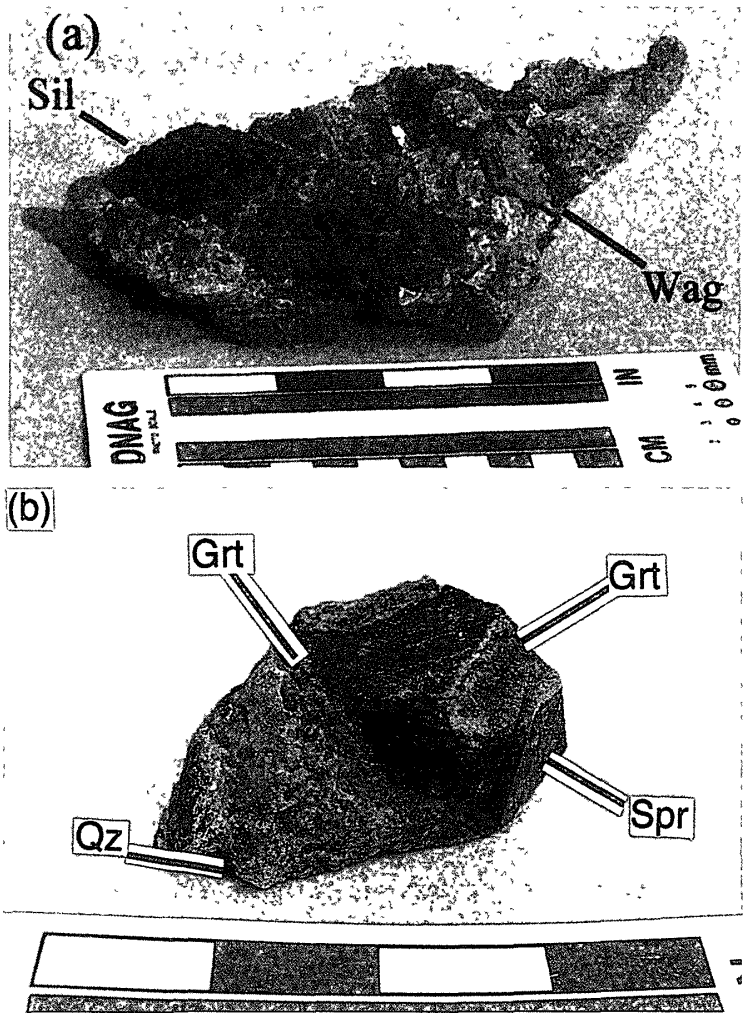

Fig 4 Photographs of specimens from "Christmas Point" pegmatites

(a) Coarse-grained sillimanite (Sil) and wagnerite (Wag) (Sample 12211)

(b) Sapphirine-khmaralite (Spr) is separated from quartz (Qz, gray) by a corona of garnet (pink, Grt) and sillimanite in the center of the specimen, quartz is missing to right of garnet-sillimanite corona on right side of specimen (Sample 12261)

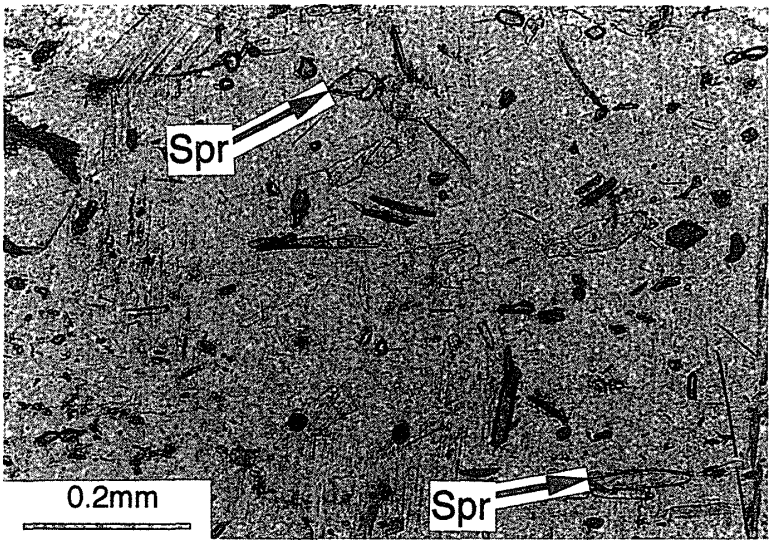

Fig 5 Photomicrograph of sapphirine inclusions (Spr) in microcline, pegmatite no 2, "Christmas Point" inclusions range from blue to nearly colorless depending on orientation Plane light (Sample 12250)

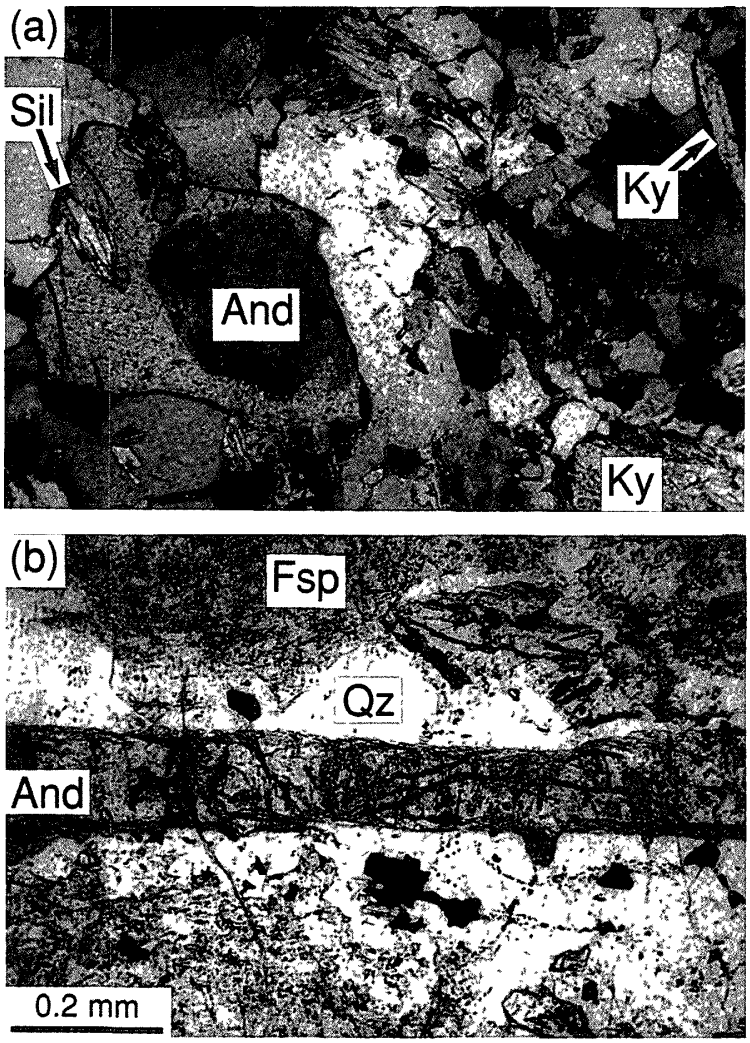

Fig 6 Photomicrographs of andalusite Scale applies to both photographs (a) Kyanite (Ky) and zoned andalusite with dark core (And) and light margin enclosing sillimanite (Sil) in a matrix of quartz containing biotite, muscovite and fibrolitic sillimanite Crossed nicols Discovery pegmatite (no 1), "Christmas Point" (Sample 12222) (b) Zoned, pink andalusite, which is isolated from turbid feldspar (Fsp) by quartz (Qz) Plane light Mt Pardoe (Sample 10508c)

Textures suggest three generations of sillimanite. (1) centimeter-sized prisms brown or gray in hand specimen, (2) prisms generally 1 to 5 mm long that are often in parallel or radiating bundles in the surinamite-bearing aggregates and coronas around sapphirine-khmaralite, and (3) fine-prismatic, locally fibrolitic, mostly with biotite, less commonly in microveinlets cutting microcline grains or around microcline grains Kyanite is a widespread if sparse constituent of the pegmatites, whereas andalusite is rare, some andalusite grains overgrow sillimanite (Fig 6a). All three aluminosilicates occur within a 1-mm^2 area in the illustrated section Near-contacts of kyanite with microcline are present in a few sections, andalusite is close to microcline in only one section

Sapphirine-khmaralite is separated from quartz by an inner corona of prismatic sillimanite and an outer one of granular garnet (with minor quartz), and is deeply embayed

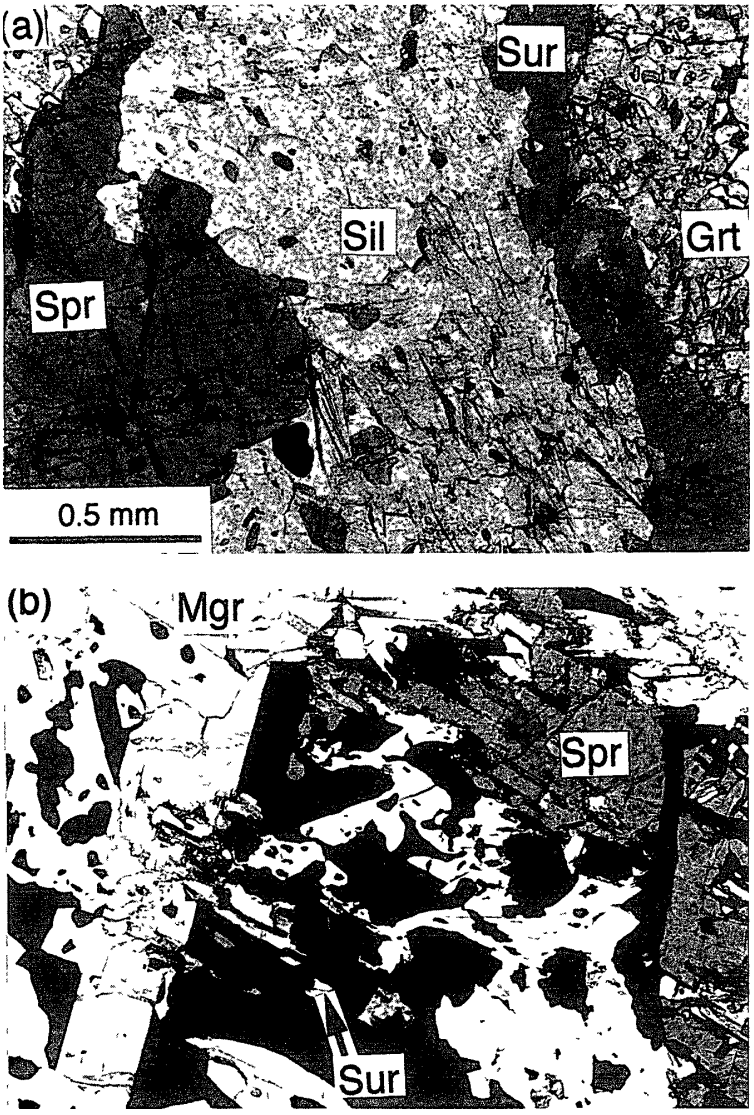

Fig 7 Photomicrographs of a sapphirine-khmaralite nodule in the second pegmatite at "Christmas Point" (Sample 12261) Plane light Scale applies to both photographs (a) Part of corona around deeply embayed sapphirine-khmaralite (Spr) showing inner sillimanite (Sil) zone and part of outer garnet (Grt) zone with surinamite (Sur) (b) Ilmenite-hematite intergrowth (opaque) with tabular musgravite (Mgr), minor surinamite (Sur) and relict sapphirine-khmaralite (Spr)

by the sillimanite corona (Fig 7a) The sapphirine-khmaralite masses are penetrated by microveinlets and aggregates consisting of hematite-ilmenite intergrowths, sillimanite, musgravite (Fig 7b), surinamite and/or corundum, the oxides are also enclosed in sapphirine-khmaralite In one sample, surinamite penetrates sapphirine-khmaralite and appears to be replacing it Surinamite also occurs along the boundary between the sillimanite and garnet coronas or within the garnet corona Where the sapphirine-khmaralite has completely reacted away, an atoll texture remains in which scattered surinamite grains stand out (Fig 8) Biotite forms a margin outside the garnet corona and microveinlets cutting it and extending into the relict sapphirine-khmaralite, fine-grained flakes of biotite are scattered in the sapphirine-khmaralite masses and both coronas

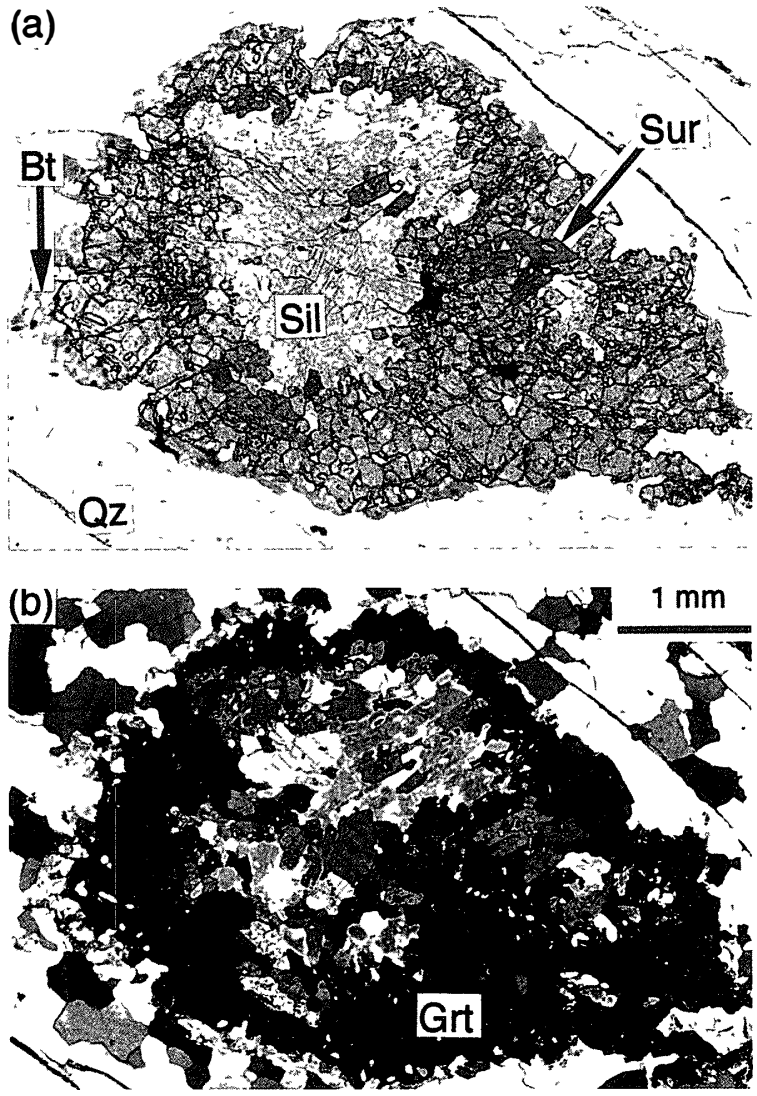

Fig 8 Photomicrographs of an atoll texture in the second pegmatite at "Christmas Point" (Sample 12264) The atoll is cored by medium-grained sillimanite aggregate (Sil) surrounded by garnet (Grt) with surinamite (Sur) Biotite forms an outer margin (Bt) (a) Plane light (b) Crossed nicols

Wagnerite is found with sapphirine-khmaralite and in the quartz matrix, where it forms flattened aggregates that wrap around the coarse sapphirine-khmaralite masses and their coronas

The surinamite-bearing aggregates, which are in part foliated, consist mostly of medium-grained quartz, surinamite, garnet, sillimanite, biotite, cordierite, apatite, and sparse orthopyroxene Cordierite develops as moats isolating garnet, surinamite and sillimanite (Fig 9), in places it forms a fine symplectitic intergrowth with quartz Textures in samples collected in 1979 suggested that orthopyroxene is coeval with garnet, surinamite and sillimanite (Grew, 1998, Fig 3b) However, in samples collected in 1999, orthopyroxene also forms selvages between cordierite and quartz (Fig 9) and thus is more likely coeval with cordierite Secondary orthoamphibole occurs in biotite in one section

An oxide veinlet in sample no 12227 consists dominantly of magnetite and subordi-

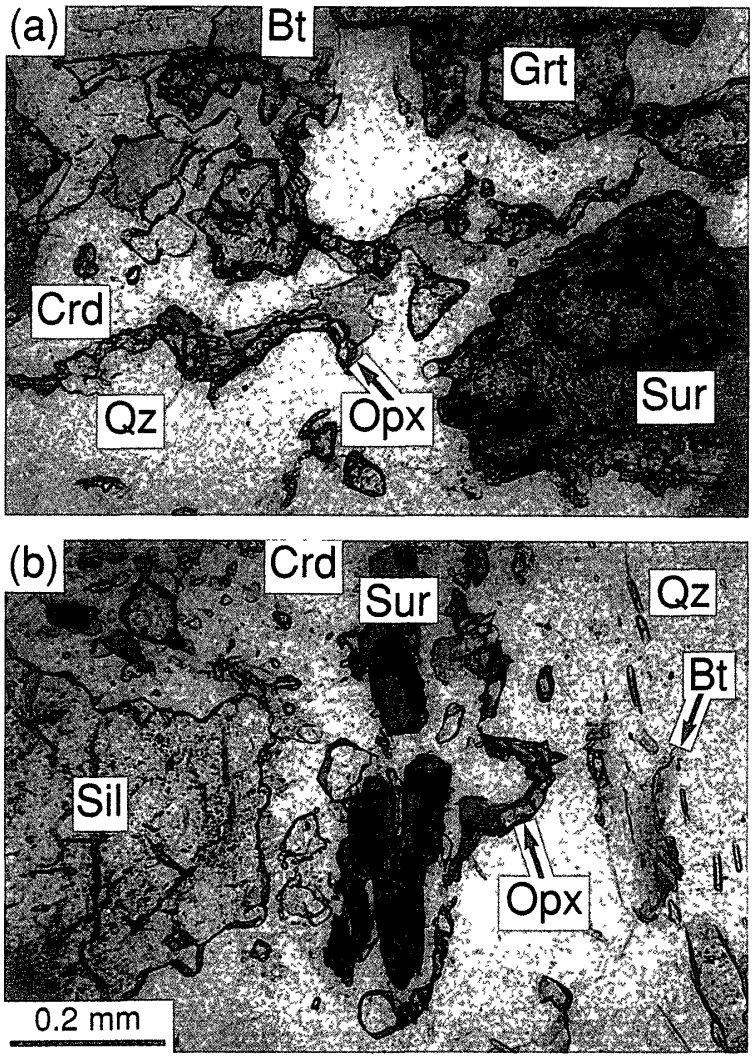

Fig 9 *Photomicrographs of orthopyroxene selvages (Opx) between cordierite (Crd) and quartz (Qz) in discovery pegmatite at "Christmas Point" Plane light Scale applies to both photographs (a) Sample 12208a (b) Sample 12210*

nate ilmenite-hematite intergrowths Grains of corundum, rutile, brown högbomite and green spinel are enclosed in magnetite, the högbomite and spinel form complex lamellar intergrowths

Overall, zircon is sparse and none was found in the coronas or surinamite-bearing aggregates

4 2 Mt. Pardoe

The pegmatites form veins about 5 cm thick that cut layering in the host granulite (Fig 2c) In hand specimen the pegmatite is light colored and contains orthopyroxene (Fig 10) grains up to 2 cm long and flattened aggregates of orange wagnerite up to 2 cm across In contrast to the "Christmas Point" pegmatite, sillimanite prisms do not exceed 1 mm in width and the coarse orthopyroxene appears to be an early formed mineral, which is partly replaced by garnet Feldspar is mostly a fine intergrowth of alkali feldspar and

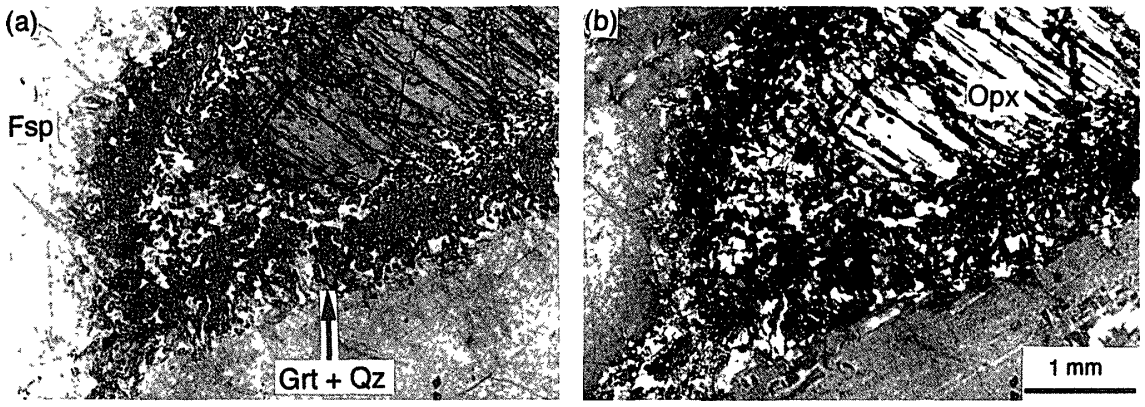

Fig 10 Photomicrographs of coarse-grained orthopyroxene (Opx) with subparallel lamellae of secondary garnet showing as high relief in (a) and black in (b) Orthopyroxene is separated from mesoperthite by corona of fine-grained garnet and quartz (Grt+Qz) Mt Pardoe, Sample 10511. (a) Plane light. (b) Crossed nicols

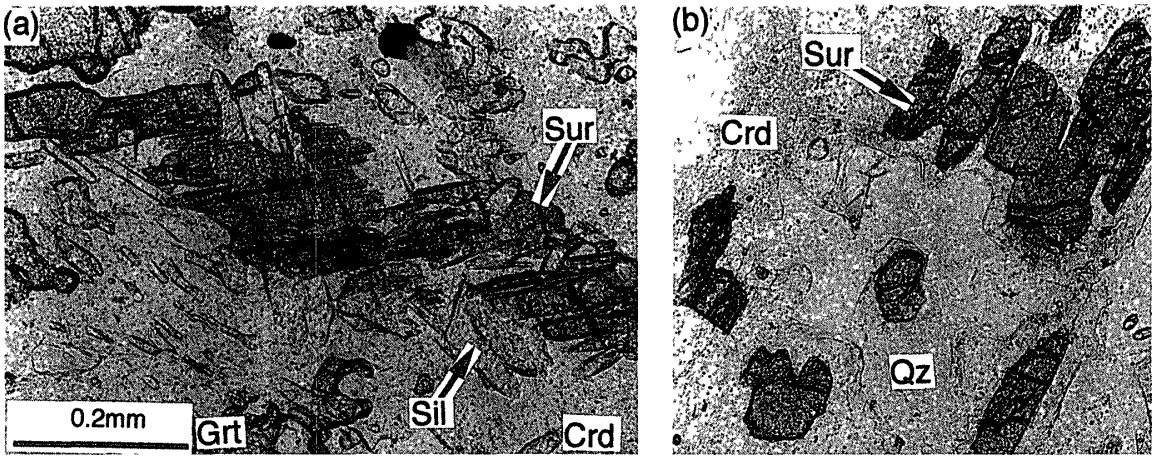

Fig 11 Photomicrographs of two different aggregates of tabular surinamite grains (Sur) in cordierite (Crd) with sillimanite (Sil) and garnet (Grt), biotite (brown) and sparse inclusions of quartz in cordierite are also present, Mt Pardoe, Sample 10510. Plane light. (a) The entire low-relief matrix is cordierite (b) This image has been darkened to emphasize that cordierite has overgrown surinamite.

plagioclase (mesoperthite); in one sample, plagioclase and K-feldspar are intergrown on relatively coarse scale suggesting recrystallization into a medium-grained perthite Cordierite shows considerable yellow pleochroism and anomalous interference colors; it locally encloses sillimanite and a fine-grained orthopyroxene, which appears to be later-formed than the coarser grains. Surinamite was found in one sample enclosed in cordierite with sillimanite, garnet and biotite (Fig 11) Kyanite and andalusite occur in either quartz or feldspar but are mostly separated from the latter by a selvage of quartz (*e.g.*, Fig. 6b) Andalusite encloses sillimanite and, and, in one case, kyanite. A selvage of apatite commonly surrounds wagnerite aggregates.

5. Mineral chemistry

5.1 Methods

Minerals from "Christmas Point", "Zircon Point" (dumortierite only) and Mt Pardoe were analyzed in carbon-coated polished thin sections by MGY for constituents with $Z > 8$ with a wavelength dispersive ARL SEMQ electron microprobe (EMP) at the University of Maine (15 kV accelerating voltage, 10 nA beam current and 3 μm spot size) Natural silicates and oxides were used as standards and data were processed with $\phi(\rho z)$ scheme in which the effect of BeO in surinamite (stoichiometric amount) and H_2O was included Sapphirine from other localities was analyzed by ESG with an ARL-EMX electron microprobe in 1980 at UCLA (method given in Grew, 1980, Barbier *et al* , 1999)

Be and B were analyzed in the same thin sections, which were gold coated, by secondary ion mass spectrometry (SIMS) with a Cameca ims 4f ion microprobe operated at the University of New Mexico (UNM) by a UNM-Sandia National Laboratories consortium Analyses were made using primary $^{16}O^-$ ions accelerated through a nominal potential of 12 5 kV A primary beam current of 10 nA was focused on the sample over a spot diameter of 20–25 μm Sputtered secondary ions were energy-filtered using a sample offset voltage of 50 V, energy window of $\pm$25 V The analyses involved repeated cycles of peak counting on ^{9}Be, ^{11}B and ^{30}Si Each spot analysis involved 10 counting cycles The signals for $^{9}Be^+$ and $^{27}Al^{3+}$ were sufficiently resolved at mass resolution of ~320 (routine conditions) to measure Be at the high concentrations found in cordierite, sapphirine-khmaralite and surinamite The analytical procedure included counting on a background position to monitor detection noise Absolute concentrations of each element were calculated using empirical relationships of measured $^{9}Be^+/^{30}Si^+$ and $^{11}B^+/^{30}Si^+$ ratios (normalized to known SiO_2 content) to element concentrations as derived from calibration measurements of surinamite (no 2292C), grandidierite (no BM1940,39), and prismatine (BM1940,39 and no 112233) standards The Be and B contents of these standards were determined from crystal structure refinement A new refinement of the site populations of surinamite in sample 2292C (Barbier, unpublished data) gives a Be/Si ratio of 0 340(1) *vs* 0 309 for the same sample from Moore and Araki (1983) The latter calibration was used for analysis of khmaralite (Barbier *et al* , 1999) The revised ratio results in a higher value for the Be content of type khmaralite

Eight measurements of the type khmaralite during five SIMS sessions gave 2 72$\pm$0 25 wt% BeO, that is, the 1sigma reproducibility is about $\pm$10% for BeO contents of ~1 wt% Reproducibility of boron measurements is comparable, six measurements of the type khmaralite during four sessions gave 0 054$\pm$0 005 wt% B_2O_3, and six measurements of the 2292C surinamite standard gave 14$\pm$1 ppm B

During analyses of sapphirine, cordierite, Al_2SiO_5 phases and surinamite in the "Christmas Point" and Mt Pardoe samples, intensity of the SIMS B signal in most cases drifted downward so that standard deviations of 10 cycles exceeded 10% of the measured value The average B contents in these minerals from "Christmas Point" and Mt Pardoe do not exceed 21 ppm and are mostly 10 ppm or less whether the intensity drifted down or not Because no downward drift was observed in the 2292C surinamite standard, which had not been carbon coated for EMPA, one possible explanation for the drift is that the carbon coat used for EMPA of minerals in the other sections could have interfered with

measurement of B at concentrations near 20 ppm B or less

5 2 Sapphirine

Sapphirine-group minerals in the "Christmas Point" pegmatites contain from 1 1 to 2 5 wt% BeO (*e.g* , Table 4) Host-rock sapphirine also contains Be, 0 01-0 07 wt% BeO at Mt Pardoe and 0 2-0 6 wt% BeO at "Christmas Point", that is, from 61 to 616 times the whole-rock Be content in the three samples for which data are available Thus, sapphirine is clearly a "sink" for Be Figure 12 shows that the trend of Be increasing with Si in the analyzed sapphirine-group minerals is consistent with incorporation of Be by the substitution $BeSiAl_{-2}$ Scatter in the points is within the $\pm 10\%$ reproducibility of BeO measurements except at low Be concentrations Variation in host-rock sapphirine compositions could be in part due to the Tschermaks substitution, $(Mg,Fe^{2+})Si(Al,Fe^{3+})_{-2}$ (Fig 12)

Cell parameters measured on a few grains of the coarse sapphirine from three samples are intermediate between those of the type khmaralite and of a comparably Fe-rich sapphirine from the Labwor Hills, Uganda (Table 5, Fig. 13) The Labwor Hills sapphir-

Table 4 Representative analyses of sapphirine and khmaralite

	Host rocks		Pegmatites		
	"Christmas Point"	Mt Pardoe	"Christmas Point"		
	Spr	Spr	Khm	Spr	Khm
No	2292M	10501*	12242	12260	12262
			wt%		
SiO_2	13 77	12 88	18 91	16 26	17 40
TiO_2	0 08	0 05	0 04	0 00	0 04
Al_2O_3	62 53	63 54	51 21	54 20	53 32
Fe_2O_3	1 52	0 73	3 36	3 56	3 75
FeO	3 78	5 39	7 79	8 54	8 27
MnO	0 00	0 00	0 03	0 04	0 00
MgO	17 64	16 85	15 86	15 43	15 32
CaO	0 00	0 00	0 00	0 02	0 00
BeO	0 61	0 07	2 31	1 07	1 84
Sum	99 94	99 50	99 51	99 13	99 94
			Formulae for 20 O and 14 cations		
Si	1 612	1 526	2 252	1 970	2 077
Ti	0 007	0 004	0 004	0 000	0 004
Al	8 627	8 875	7 188	7 736	7 502
Fe^{3+}	0 134	0 065	0 301	0 325	0 337
Fe^{2+}	0 370	0 534	0 775	0 865	0 826
Mn	0 000	0 000	0 003	0 004	0 000
Mg	3 078	2 976	2 816	2 787	2 727
Ca	0 000	0 000	0 000	0 003	0 000
Be	0 171	0 020	0 661	0 311	0 527
Sum	14 000	14 000	14 000	14 000	14 000
$X(Mg)$	0 893	0 848	0 784	0 763	0 767

Note Na and K are below detection FeO and Fe_2O_3 were calculated assuming ideal stoichiometry $X(Mg)=Mg/(Mg+Fe^{2+})$ *Also Na_2O 0 02(0 01) wt%

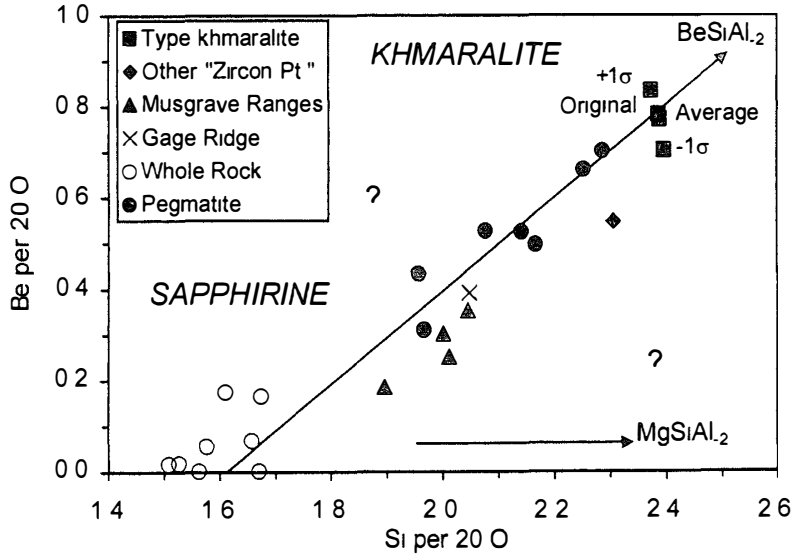

Fig 12 Beryllium and silicon contents of sapphirine and khmaralite "Original" refers to the Be and Si contents reported for the type khmaralite by Barbier et al (1999) adjusted for a revision in the Be/Si ratio of the surinamite standard used for SIMS The other points for type khmaralite refer to the average and ± 1 standard deviation of eight SIMS analyses carried out concurrently with the other samples Sources of electron microprobe data type khmaralite (Barbier et al, 1999), Musgrave Ranges (Grew, unpublished data on D R Hudson's sample 14820), Gage Ridge (no 2045A, Grew, 1981), other "Zircon Point" (sample 2234L/2, Grew, 1981, Grew and Yates, unpublished data) The boundary between sapphirine and khmaralite is suggested by the appearance of superstructure reflections in electron diffraction patterns of no 12262 Whole rock samples are from both "Christmas Point" and Mt Pardoe, the pegmatite samples are all from "Christmas Point"

ine is presumed to contain negligible Be, Grew *et al* (1990) found no Be in sapphirine in another sample from this locality In principle, at constant total Fe content, cell volume should decrease monotonically with increasing Si and Be substitution for tetrahedral Al (*e.g*, Christy, 1988) Deviations from the predicted trend are most likely due to compositional heterogeneity, which was found by analyzing several points in no 12262, consequently, the grains used for X-ray diffraction could have differed somewhat in composition from the analyzed grains in the same sample

Electron diffraction patterns of no 12262 show superstructure reflections characteristic of khmaralite (Table 5) Given the high BeO contents of the analyzed spots of nos 12261 and 12242, parts of these samples could be khmaralite as well, *i.e*, the "Christmas Point" sapphirine-group minerals are mixtures of sapphirine and khmaralite

B contents of the analyzed sapphirine-khmaralite from the host rocks and "Christmas Point" pegmatite range $<1-11$ ppm, whereas khmaralite from the "Zircon Point" pegmatite contains 0 05-0 13 wt% B_2O_3

5 3 Surinamite

BeO of the analyzed surinamites from "Christmas Point" range from 3 9 to 5 2 wt% and average 4 36±0 40 wt% (*e g*, Table 6), the average for surinamite in nos 2234L/3 and

Table 5. Comparison of cell parameters with structural state and compositional features of khmaralite and beryllian sapphirine

Sample no	*a* (Å)	*b* (Å)	*c* (Å)	*β* (°)	ΣFeO (wt%)	2 x *a* superstructure
2234L/3	9 900(8)	14 369(2)	11 254(1)	125 5(1)	10 06	Yes
11262	9 925(3)	14 403(3)	11 273(2)	125 5(1)	10 96, 11 65, 11 23	Yes, weak
11260a	9 940(4)	14 421(4)	11 279(3)	125 5(1)	11 75	Not seen
11261	9 946(3)	14 425(3)	11 285(2)	125 5(1)	10 81	Not seen
Labwor	9 985(5)	14 480(6)	11 314(4)	125 44(4)	12 36	—

Note Data on 2234L/3, type khmaralite from "Zircon Point", is taken from Barbier *et al* (1999) The cell dimensions were determined by least-squares refinement of 25 to 30 reflections recorded on photographic film in a Guinier-Haegg powder X-ray camera, scanned with a computer-controlled digital scanner, and calibrated with Si powder as internal standard The esd's are given in parentheses The presence or absence of a superstructure was determined by electron diffraction in a Philips CM-12 transmission electron microscope operating at 120 keV, the superstructure is not detectable by powder X-ray diffraction The data on Labwor sapphirine are taken from Sahama *et al* (1974)

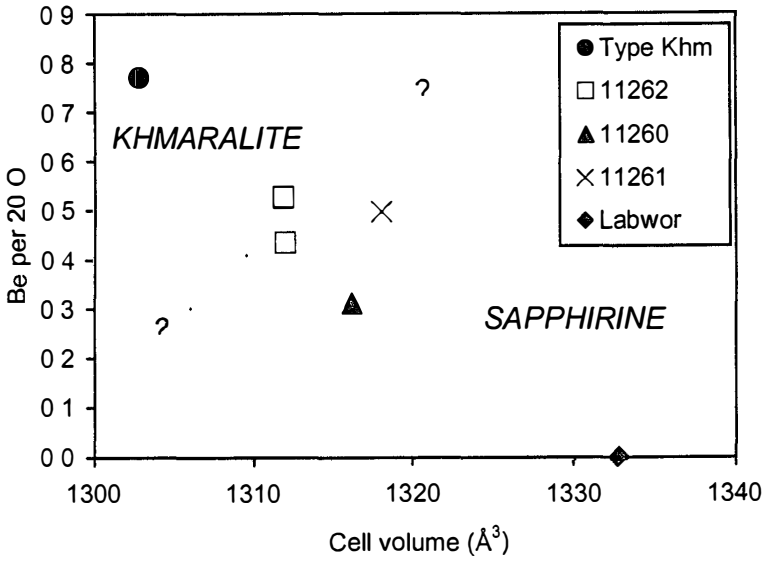

Fig 13 Relationship between cell volume for Z = 4 (Table 5) and BeO content in khmaralite and sapphirine Position of the boundary between sapphirine and khmaralite is suggested by the appearance of superstructure reflections in electron diffraction patterns of no 12262

2234L/4 from "Zircon Point" is 4 53±0 14 wt% BeO Both values lie within the 1sigma reproducibility of ±10% of the ideal BeO content of surinamite (~4 4–4 5 wt%) Only one analysis significantly deviates from the average 5 19 wt% on one grain in no 12242 Consequently, the stoichiometric BeO value is assumed for calculating formulae

B contents of the analyzed surinamite from "Christmas Point" range 4–15 ppm, whereas surinamite from "Zircon Point" contains 0 09–0 15 wt% B_2O_3 Fractionation of B into surinamite relative to sapphirine-khmaralite is only evident in the "Zircon Point"

Table 6 Selected analyses of surinamite

	"Christmas Point"					Mt Pardoe
	12210	12242	12261	12262	2292C	10510B
			wt%			
SiO_2	32 22	31 78	31 72	31 42	31 32	32 43
P_2O_5	0 26	—	—	—	0 33	—
TiO_2	0 00	0 00	0 04	0 03	0 00	0 05
Al_2O_3	34 78	34 33	34 31	35 05	32 82	36 19
Fe_2O_3	3 87	5 62	4 25	5 84	5 59	2 13
FeO	5 91	5 79	7 80	5 45	9 14	4 93
MnO	0 21	0 08	0 00	0 02	0 17	0 06
MgO	18 41	18 01	16 85	18 01	16 08	18 93
CaO	0 10	0 02	0 09	0 00	0 08	0 07
BeO(m)	4 32	4 78	4 04	4 29	4 44	—
BeO(c)	4 54	4 50	4 46	4 52	—	4 55
Sum	100 28	100 13	99 51	100 35	99 97	99 35
	Formulae per 16 O and 11 cations					
Si	2 956	2 936	2 961	2 894	2 944	2 970
P	0 020	—	—	—	0 027	—
Ti	0 000	0 000	0 003	0 002	0 000	0 004
Al	3 760	3 738	3 775	3 805	3 636	3 906
Fe^{3+}	0 267	0 391	0 299	0 404	0 395	0 147
Fe^{2+}	0 454	0 447	0 609	0 421	0 719	0 378
Mn	0 016	0 006	0 000	0 002	0 014	0 005
Mg	2 518	2 481	2 345	2 473	2 254	2 584
Ca	0 009	0 002	0 009	0 000	0 008	0 007
Be(m)	—	—	—	—	1 002	—
Be(c)	1 000	1 000	1 000	1 000	—	1 000
Sum	11 000	11 000	11 000	11 000	11 000	11 000
X(Mg)	0 847	0 847	0 794	0 854	0 758	0 872

Note Na and K are below detection (m)—measured (c)—calculated FeO, Fe_2O_3 and BeO(c) were calculated assuming ideal stoichiometry Sums include only BeO(c) and Be(c) except for 2292C $X(Mg)=Mg/(Mg+Fe^{2+})$ No 12210 is surrounded by cordierite (*cf* Fig 9b) No 12242 is adjacent to khmaralite No 12261 is in garnet corona No 12262 is near khmaralite, corundum and musgravite No 2292C is from Sur-Grt-Sil aggregate Be was determined by crystal structure refinement (Barbier, unpublished data) No 10510B is surrounded by cordierite

sample richest in B and containing dumortierite (no 2234L/3)

P_2O_5 contents of three analyzed samples range from 0 26 to 0 33 wt%

5 4 *Al_2SiO_5 phases*

Sillimanite differs in Fe_2O_3 content from one locality to another, ranging from 0 3 wt% in the host rocks at Mt Pardoe to 1 1 wt% in the pegmatites at "Christmas Point" (*e g*, Grew, 1981, this paper, Table 7) Fe_2O_3 of associated Al_2SiO_5 phases increases Ky < And (rims) < Sil in one sample from "Christmas Point" (no 12222) Zoning in andalusite in this sample reflects Fe_2O_3 and MgO contents, the inner zones that appear dark in polarized

Table 7 Selected analyses of Al_2SiO_5 minerals

	"Christmas Point"				Mt Pardoe
	Sil	Ky	And*	And**	Sil
		12222 (1 mm² area) wt%			10510B
SiO_2	37 00	36 95	36 42	36 34	36 72
TiO_2	0 00	0 00	0 00	0 05	0 00
Al_2O_3	61 70	62 05	62 27	60 11	62 31
Fe_2O_3	1 03	0 67	0 90	2 47	0 38
MgO	0 00	0 00	0 05	0 25	0 00
Sum	99 73	99 67	99 65	99 22	99 41
	Formulae per 5 O				
Si	1 004	1 002	0 990	0 997	0 998
Ti	0 000	0 000	0 000	0 001	0 000
Al	1 974	1 983	1 994	1 944	1 995
Fe^{3+}	0 021	0 014	0 018	0 051	0 008
Mg	0 000	0 000	0 002	0 010	0 000
Sum	2 999	2 999	3 004	3 004	3 001

Note All Fe as Fe_2O_3 Mn, Ca, Na and K below detection *Outer zone **Inner zone, F, Cl and P below detection

light (Fig 6a) contain more of both constituents SIMS analyses of the inner zone of andalusite (no 12222) and of a sillimanite (no 10501) gave 1 and 2 ppm Be and 1 and 21 ppm B, respectively, the Be values are maxima because of the possible interference of triply charged Al at such low concentrations of Be

5.5. Oxides

Musgravite and spinel from "Christmas Point" contain Zn and minor Ga, but negligible Cr (Table 8), a similar signature is characteristic of musgravite from "Zircon Point" (Grew, 1981, Schmetzer, 1983) Assuming ideal stoichiometry of $(Mg,Fe^{2+},Zn)_2(Al,Fe^{3+},Ga)_6BeO_{12}$, we calculate the "Christmas Point" musgravite to contain some Fe^{3+}, whereas the "Zircon Point" musgravite is calculated to contain none

Magnetite in sample no 12227 is nearly end-member Fe_3O_4 with 0 2–0 3 wt% Al_2O_3, ~0 1 wt% Ga_2O_3, <0 1 wt% MgO and negligible TiO_2, SnO_2, Cr_2O_3, MnO and ZnO Back-scattered electron images of hogbomite-spinel intergrowths enclosed in magnetite show a dominant (host) phase of lower average atomic number containing lamellae of higher average atomic number oriented in three directions The host is either spinel or Sn-poor högbomite (col 4–5, Table 8), whereas lamellae are either Sn-rich högbomite (col 6, Table 8) or högbomite richer in Zn Högbomite formulae were calculated on a 30 O+ 2(OH) basis assuming the 8H polysome (Gatehouse and Grey, 1982) Thomas Armbruster and Clivia Hejny (personnal communication, 2000) report that preliminary results show the 8H polysome to be dominant in this högbomite The Sn-bearing lamallae could be submicroscopic layered intergrowths of högbomite and nigerite as suggested by Petersen *et al* (1989) for similar Sn-bearing hogbomite from Manitouwadge, Canada

Table 8 Selected analyses of oxides from "Christmas Point"

	Mgr 12242	Mgr 12262	Spl 12242*	Spl 12227	Hog 12227	Hog 12227**
			wt%			
TiO_2	0 05	0 00	0 00	0 28	5 67	6 06
SnO_2	—	—	—	0 29	0 30	6 63
Al_2O_3	67 49	68 18	59 77	60 45	59 34	57 24
Ga_2O_3	0 40	0 33	0 28	0 48	1 79	0 94
Fe_2O_3	1 59	2 03	1 52	0 22	7 80	0 11
FeO	8 37	10 30	18 30	17 83	12 45	14 72
MnO	0 00	0 00	0 03	0 13	0 11	0 09
MgO	11 09	11 54	8 36	8 99	6 45	6 34
ZnO	4 77	2 10	10 95	10 95	4 49	5 03
BeO	5 62	5 70	—	—	—	—
H_2O	—	—	—	—	1 43	1 38
Sum	99 39	100 16	99 21	99 62	99 81	98 54
	Formula for given O and total cations					
O	12	12	4	4	32	32
Ti	0 003	0 000	0 000	0 006	0 896	0 994
Sn	—	—	—	0 003	0 025	0 577
Al	5 887	5 873	1 963	1 969	14 686	14 709
Ga^{3+}	0 019	0 015	0 005	0 009	0 240	0 132
Fe^{3+}	0 089	0 111	0 032	0 005	1 232	0 018
Fe^{2+}	0 518	0 629	0 426	0 412	2 187	2 685
Mn	0 000	0 000	0 001	0 003	0 019	0 017
Mg	1 224	1 257	0 347	0 370	2 018	2 059
Zn	0 261	0 113	0 225	0 223	0 696	0 810
Be	1 000	1 000	—	—	—	—
Sum	9 000	9 000	3 000	3 000	22 000	22 000
H	—	—	—	—	2 000	2 000
X(Mg)	0 70	0 67	0 45	0 47	0 48	0 43

Note FeO, Fe_2O_3, BeO and H_2O were calculated assuming ideal stoichiometry Si and Cr are below detection $X(Mg)=Mg/(Mg+Fe^{2+})$ *SiO_2 0 07(0 06) wt% **SiO_2 0 16(0 14) wt% No 12227 grains are enclosed in Mgt Sn-rich hogbomite forms a lamella in Sn-poor hogbomite

5.6 Miscellaneous ferromagnesian silicates

Some cordierite contiguous to surinamite (*e.g*, Fig 9b) is richer in Na, K, Ca and has a lower Al/Si ratio than cordierite associated with other minerals (Table 9) SIMS analysis implies that these features are due to incorporation of Be by the substitution (Na, $K,Ca_{0.5})Be(\square Al)_{-1}$ Garnet is magnesian almandine with little Ca and Mn (Table 10)

Orthopyroxene in selvages between quartz and cordierite or garnet in the two "Christmas Point" pegmatites contains only 1 69–2 06 wt% Al_2O_3 (*e g*, Table 11, col 1) despite the presence of sillimanite nearby (*e g*, Fig 9b) In contrast, orthopyroxene in the Mt Pardoe pegmatite is fairly aluminous, the medium-grained more so, 6 61–6 69 wt% Al_2O_3 (*e.g*, Table 11, col 2) than finer-grained enclosed in cordierite in the same section, 5 59–5 91 wt% Al_2O_3 (*e.g*, Table 11, col 3)

Table 9 Selected analyses of cordierite

	"Christmas Point"		Mt Pardoe	
	12210	12240	10510B-1	10510B-2
		wt%		
SiO_2	48 89	49 17	48 28	47 31
Al_2O_3	30 89	34 39	32 24	30 75
FeO	3 38	4 66	2 93	2 98
MnO	0 06	0 04	0 00	0 00
MgO	11 25	10 20	11 49	11 60
CaO	0 03	0 00	0 02	0 13
Na_2O	1 21	0 07	0 23	0 45
K_2O	0 00	0 01	0 02	0 14
BeO	1 00	—	—	0 64
Sum	96 70	98 55	95 21	94 01
		Formula per 18 O		
Si	5 011	4 962	5 012	4 981
Al	3 731	4 091	3 945	3 816
Be	0 246	—	—	0 161
Fe	0 290	0 394	0 255	0 263
Mn	0 005	0 003	0 000	0 000
Mg	1 718	1 535	1 778	1 821
Ca	0 003	0 000	0 003	0 015
Na	0 239	0 014	0 045	0 091
K	0 000	0 001	0 002	0 019
Sum	11 244	11 000	11 040	11 166
X(Mg)	0 856	0 796	0 875	0 874

Note All Fe as FeO Ti is below detection $X(Mg)=Mg/(Mg+Fe)$ No 12210 is around surinamite (*cf* Fig 9b) No 12240 is in Grt-Sil±Sur aggregate No 10510B-1 is with Opx and Sil No 10510B-2 is around surinamite

Coarse-grained, brown biotite is Ti-rich (Table 12, col. 1), whereas secondary biotite, which is finer-grained, paler in color and commonly pleochroic in green as well as brown, contains negligible Ti (Table 12, col 2), both varieties contain substantial F and Cl

Orthoamphibole is Al-poor anthophyllite (Table 12)

5.7. Chain silicates from the Mt. Charles pegmatite

Coarse-grained hornblende, which is mantled and partially replaced by an orthopyroxene+plagioclase symplectite (Grew, 1998, Fig 5), is among those hornblendes richest in F and K_2O (Leake, 1968, Deer *et al.*, 1997). Most F-rich hornblendes from elsewhere are more magnesian except for a few hastingsites, many are pargasites from calc-silicate rocks (*e.g* Petersen *et al* , 1982) Back-scattered-electron (BSE) images of the hornblende show lamellae, some very fine, throughout the hornblende, these could be the cause for schiller, which is best seen in a thin section viewed with the naked eye In BSE images, the coarsest lamellae are striped at an angle; this striping results from an intergrowth of orthopyroxene with augite (Table 11) and minor actinolite

Table 10 Representative analyses of garnet

	"Christmas Point"			Mt Pardoe
	12240	12242	12260	10510B
		wt%		
SiO_2	39 75	40 18	40 29	40 20
Al_2O_3	22 84	22 31	22 22	22 13
FeO	25 40	24 66	24 63	24 30
MnO	0 75	0 46	0 22	0 28
MgO	10 80	11 99	12 49	12 55
CaO	0 52	0 49	0 48	0 69
Sum	100 07	100 09	100 33	100 16
		Formulae per 12 O		
Si	3 011	3 028	3 026	3 024
Al	2 039	1 982	1 967	1 962
Fe	1 609	1 555	1 547	1 529
Mn	0 048	0 030	0 014	0 018
Mg	1 219	1 347	1 398	1 408
Ca	0 042	0 039	0 039	0 056
Sum	7 969	7 981	7 991	7 996
X(Mg)	0 431	0 464	0 475	0 479

Note All Fe as FeO $X(Mg)=Mg/(Mg+Fe)$ Ti, Na, and K are below detection No 12240 is near Opx in Sur-bearing aggregate Nos 12242 and 12260 are in coronas No 10510B is near Sur

5 8. *Dumortierite*

The only boron mineral in the beryllium pegmatites is very sparse, purple dumortierite in grains and aggregates up to 0 25 mm across with musgravite, biotite and khmaralite in sample 2234L/3 from "Zircon Point" Electron microprobe analysis gave SiO_2 31 15, TiO_2 2 10, Al_2O_3 57 08, FeO 0 62, MgO 1 54, CaO 0 01 and values calculated from stoichiometry are B_2O_3 6 08, H_2O 1 18, which sums to 99 78 wt% and corresponds to $Al_{6\,41}Fe_{0\,05}Mg_{0\,22}Ti_{0\,15}BSi_{2\,97}(OH)_{0\,75}$, Sn, Nb, Ta, P, Mn are below detection A SIMS analysis gave 5 3 wt% B_2O_3, but the analyzed grain was too narrow to fully accommodate the ion probe beam, and thus this value was not used to calculate the formula

5 9. *Relationships among the minerals*

In general, Mg-Fe^{2+} fractionation is such that X(Mg) decreases cordierite $\geq$ surinamite > sapphirine-khmaralite > orthopyroxene, musgravite > garnet $\geq$ spinel We consider this sequence to represent an equilibrium Mg-Fe^{2+} distribution even though one mineral is commonly replacing another, distribution equilibrated as replacement proceeded This sequence is consistent with sequences reported elsewhere for surinamite (Baba *et al*, 1999, 2000), cordierite, sapphirine, orthopyroxene and garnet

The proportion of ferric iron in rock-forming minerals, $X(Fe^{3+})=Fe^{3+}/(Fe^{3+}+Fe^{2+})$, is a measure of the extent to which the rock containing these minerals is oxidized (*e g*, Grew *et al*, 1999) The values of $X(Fe^{3+})$ calculated from stoichiometry in musgravite, sapphirine and surinamite increase regularly with the Fe^{3+} content of sillimanite with surinamite having a higher $X(Fe^{3+})$ than associated sapphirine-khmaralite

Table 11 Selected analyses of pyroxene.

	"Christmas Point"	Mt Pardoe		Mt Charles	
	Opx	Opx	Opx	Opx	Cpx
	12240	10510B-1	10105B-2	2098E	
			wt%		
SiO_2	53 89	51 56	51 47	52 05	52 19
TiO_2	0 00	0 07	0 06	0 10	0 18
Al_2O_3	1 69	6 69	5 59	0 52	1 42
FeO	19 18	15 85	17 46	26 14	8 95
MnO	0 16	0 00	0 04	1 53	0 52
MgO	24 97	25 73	25 03	19 54	13 90
CaO	0 02	0 02	0 02	0 47	22 17
Na_2O	0 00	0 00	0 00	0 00	0 59
K_2O	0 00	0 00	0 00	0 00	0 02
Sum	99 91	99 92	99 66	100 34	99 94
			Formula per 6 O		
Si	1 969	1 856	1 873	1 977	1 955
Ti	0 000	0 002	0 002	0 003	0 005
Al	0 073	0 284	0 240	0 023	0 063
Fe	0 586	0 477	0 531	0 830	0 280
Mn	0 005	0 000	0 001	0 049	0 016
Mg	1 360	1 381	1 358	1 107	0 776
Ca	0 001	0 001	0 001	0 019	0 890
Na	0 000	0 000	0 000	0 000	0 043
K	0 000	0 000	0 000	0 000	0 001
Sum	3 994	4 000	4 005	4 008	4 030
X(Mg)	0 699	0 743	0 719	0 571	0 735

Note All Fe as FeO $X(Mg)=Mg/(Mg+Fe)$ No 12240 is a selvage between garnet and quartz No 10510B-1 is medium-grained (1 2 mm) No 10105B-2 is fine-grained (0 1 mm) with sillimanite in cordierite No 2098E are both lamellae in hornblende

(Fig 14) Overall, the two "Christmas Point" pegmatites are more oxidized than the pegmatites at Mt Pardoe and "Zircon Point" Two of the three host rocks in which sapphirine and sillimanite were analyzed from "Christmas Point" (2292F, 2282G) are also relatively oxidized compared to two host rocks similarly analyzed from Mt Pardoe

6. Evolution of the pegmatites

6.1. Intrusion

Critical to understanding the evolution of the beryllium pegmatites is relating their formation to the sequence of tectonothermal events that affected the host rocks (Table 13) Discussion has centered around the question whether the Late Archean pegmatites, including the beryllium pegmatites, were associated with the ultrahigh temperature event (Scenario 1) or with a discrete event following the ultrahigh-temperature event at substantially lower temperature (650–700°C, 5–8 kbar, Scenario 2) The principal structural argument for the Late Archean pegmatites being younger than the ultrahigh-temperature tectonothermal event is based on crosscutting relationships and the relatively undeformed appearance

Table 12 Analyses of biotite and amphibole

	"Christmas Point"			Mt Charles
	Bt	Bt	Oam	Hbl
	12269	12210	12210	2098E
	wt%			
SiO_2	37 51	40 15	56 42	42 75
TiO_2	3 22	0 11	0 00	2 00
Al_2O_3	14 99	15 15	1 21	10 35
FeO	14 90	11 82	18 07	14 34
MnO	0 00	0 00	0 34	0 31
MgO	15 31	19 17	22 14	12 76
CaO	0 00	0 02	0 03	11 26
Na_2O	0 15	0 15	0 05	1 66
K_2O	9 63	9 14	0 00	1 81
F	1 78	2 24	0 61	1 81
Cl	0 99	1 42	0 06	0 39
H_2O	2 94	2 71	1 82	1 04
O=F, Cl	−0 97	−1 26	−0 27	−0 85
Sum	100 45	100 83	100 49	99 62
	Formulae per given O			
O	24	24	23	23
Si	5 578	5 822	7 938	6 431
Ti	0 360	0 012	0 000	0 226
Al	2 628	2 590	0 201	1 835
Fe	1 853	1 434	2 127	1 804
Mn	0 000	0 000	0 041	0 039
Mg	3 395	4 144	4 644	2 861
Ca	0 000	0 003	0 005	1 815
Na	0 044	0 042	0 014	0 484
K	1 827	1 691	0 000	0 347
Sum cations	15 683	15 737	14 969	15 841
F	0 835	1 025	0 273	0 861
Cl	0 250	0 350	0 015	0 100
OH	2 915	2 625	1 711	1 039
Sum anions	4 000	4 000	2 000	2 000
XMg	0 647	0 743	0 686	0 613

Note All Fe as FeO XMg=Mg/(Mg+Fe) H_2O calculated from F+Cl+OH=4 (biotite), =2 (amphibole) No 12269 is coarse-grained (>2 cm) Bt in no 12210 is fine-grained (0 10–0 15 mm) Oam in no 12210 is anthophyllite next to biotite

of the pegmatites (*e.g*, Fig 2) Bodies of the Late Archean pegmatites lie at high angles to structures related to deformation considered coeval with the ultrahigh-temperature event In addition, Grew (1981) described a narrow aureole of discoloration in the host rock at the contact of a Late Archean pegmatite, an observation consistent with post-metamorphic emplacement Sheraton *et al* (1987) and Harley and Black (1997) cited geochronological data in support of Scenario 2 (*cf* Grew, 1998)

However, we find compelling Sandiford and Wilson's (1984) conclusion that the Late Archean pegmatites are related to boudinage during D_2, they specifically state that no

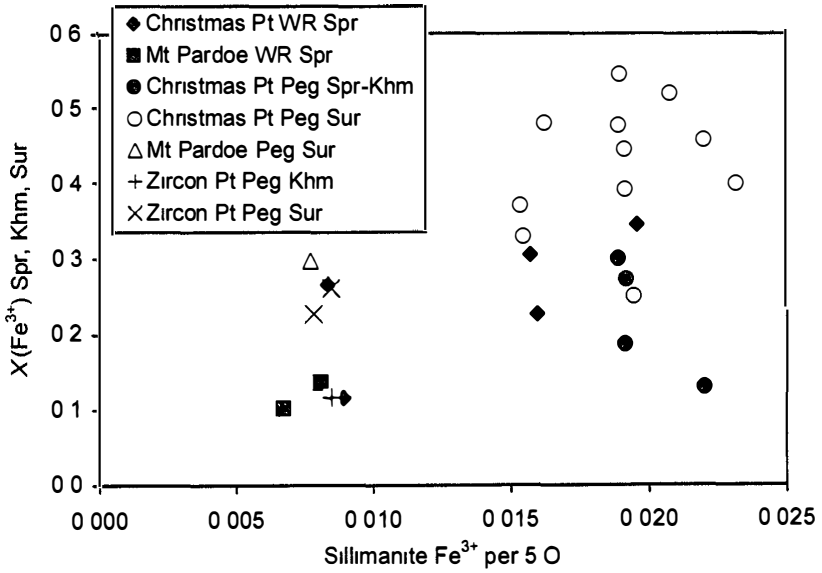

Fig 14 Ferric iron contents of associated sillimanite, surinamite, sapphirine and khmaralite $X(Fe^{3+}) = Fe^{3+}/(Fe^{3+} + Fe^{2+})$, *WR-whole rock, Peg-pegmatite, Spr-sapphirine, Khm-khmaralite, Sur-surinamite Sources of data are Grew (1981 and unpublished data), Barbier et al (1999) and this paper (Tables 4, 6, 7 and unpublished data)*

pegmatites were found between D_3 boudins in the Khmara Bay area. The *en echelon* array at "Christmas Point" appears to be the result of boudinage during D_2 of the quartz granulite layer, which may have been more competent than enclosing garnet gneiss. Sandiford and Wilson (1984) suggested that anatectic melt could have moved in to fill inter-boudin spaces and crystallize as peraluminous pegmatite, that is, the pegmatites intruded while the host rocks were still being deformed Taken together, the apparently conflicting observations on the structural relationships could be reconciled had the Late Archean pegmatites been intruded after the peak of metamorphism in the waning stages of deformation, but that the time interval between metamorphic peak and pegmatite intrusion was relatively small Table 13 is arranged to illustrate this relationship In summary, we conclude that the pegmatites formed by melting during the ultrahigh-temperature metamorphism, and were emplaced at high temperatures relatively soon after peak conditions had been attained Temperature conditions for crystallization of the Khmara Bay area host rocks during Metamorphism-1 were first estimated to be 900-960°C at 7-10 kbar (Harley, 1985a), more recent estimates are even higher, 1000-1100°C at 9-11 kbar (*e.g*, Sandiford and Powell, 1986, Harley, 1998a, b)

The interpretation in Table 13 differs from the three-stage evolution for the beryllium pegmatites proposed by Grew (1998) whereby the pegmatites were emplaced on the prograde path under conditions where cordierite was stable A beryllian cordierite precursor was presumed because the beryllium-rich assemblages have a bulk composition close to beryllian cordierite, albeit poorer in silica Grew's (1998) proposed evolution was consistent with the formation of a cordierite precursor to sapphirine+quartz on the prograde path (Motoyoshi and Hensen, 1989) This evolution also appeared to apply to the pegmatite from Mt. Charles in which hornblende had crystallized at moderate tempera-

Table 13 Stages of mineral formation in the Late Archean pegmatites and host rocks

		Ultrahigh-temperature Event		Metamorphism -2	Metamorphism -3, -4
		Metamorphism -1	Pegmatite intrusion		
Scenario 1		D_2-M_1 at ~2475 Ma		post D_2-M_1	D_4-M_3 and D_5-M_4 between ~1000 and ~500 Ma
Scenario 1'				**Separate event**	
Scenario 2		D_2-M_2 at ~2837 Ma	D_3-M_3 at ~2475 Ma	post D_2-M_2 & pre D_3-M_3	M_4 and M_5 after ~1100 Ma
"Christmas Point" and "Zircon Point"					
Al_2SiO_5		Sil (1)	Sil (1)	Sil (2)	Sil & fibrolite (3), Ky, And
Sapphirine and its breakdown products	Host rock	Spr+Qtz	—	Spr+Qtz→Sil (Crn)±Opx± Grt	Oam, Crd
	Pegmatite	—	Spr-Khm+Qtz	Spr-Khm+Qtz →Sil (Mgr, Cb) +Sur+Grt	Sur+Grt+Sil +Qtz→Crd± Opx
Alkali feldspar		disordered Kfs		—	Kfs→Mc
Other localities					
Mt Pardoe pegmatite		—	Opx (1), Grt (1)	Sur, Opx (2), Sil, Grt (2)	Crd
Mt Charles pegmatite		—	Hbl, Opx (1)	Hbl→Pl+Opx (2)	—

Note Scenario 1 is from Sandiford (1985a, b), Sandiford and Wilson (1984) and Grew (1998), Scenario 2 is from Black *et al* (1983), Harley and Black (1997) and Harley (1985a, b) Minerals in parentheses formed in isolation from quartz, numbers in parentheses refer to generation Bold indicates the new interpretation outlined in the present paper

tures on the prograde path

The discovery of coarse-grained sapphirine-khmaralite at "Christmas Point" on JARE-40 means that there is no longer any need either to presume a cordierite precursor for the Be-rich aggregates characteristic of the pegmatites or to propose pegmatite intrusion on the prograde path, which contradicts the structural relationships discussed above Several lines of evidence indicate that the precursor was sapphirine-khmaralite The characteristic assemblage of the aggregates, Sur+Grt+Sil, is the same as the corona assemblages replacing sapphirine-khmaralite masses The atoll texture (Fig. 8) represents an intermediate stage between sapphirine-khmaralite surrounded by relatively narrow (*i.e*, a few millimeters thick, Fig 4b) sillimanite-garnet-surinamite coronas and the Be-rich aggregates in which all evidence for relict sapphirine-khmaralite and the coronal texture has been obliterated The presence of sapphirine inclusions in microcline implies the early presence of sapphirine in both pegmatites at "Christmas Point", although no coarse-grained sapphirine mineral remains in the discovery pegmatite (no 1)

Sapphirine-khmaralite in the pegmatites is interpreted to have crystallized from a melt An alternative interpretation is that the sapphirine-khmaralite is entrained restitic material

However, the pegmatitic sapphirine-khmaralite is not only much coarser grained than host-rock sapphirine, but also contains more Be and Fe Possibly the pegmatitic sapphirine crystallized from seeds of restitic origin, but its present size and composition must have been largely determined by interaction with the melt The possibility of magmatic sapphirine in general has been demonstrated experimentally in the CaO-MgO-Al_2O_3-SiO_2 (P=20–30 kbar, $T \geq 1390$°C, Liu and Presnall, 1990, 2000, Milholland and Presnall, 1998) and MgO-Al_2O_3-SiO_2 systems (P=1 bar, $T > 1400$°C, Foster, 1950, Keith and Schairer, 1952). In addition, its occurrence in a partially melted Al-rich xenolith at $P \approx 3.5$ kbar and T=1100–1180°C has been suggested by Harley and Christy (1995). Given the peak temperatures of ~1100°C estimated for the ultrahigh-temperature event by Harley (1998a), formation of magmatic sapphirine in the Napier Complex pegmatite appears to be possible, even at temperatures slightly below peak, as proposed above Whether quartz was a liquidus phase with sapphirine is more debatable In the experiments on the MgO-Al_2O_3-SiO_2 system, liquidus sapphirine was found in association with spinel, mullite, cordierite and/or corundum; in the xenolith, it was found with spinel, enstatite, cordierite, alkali feldspar and phlogopite, a SiO_2 phase was not reported in either case Thus, it is possible that quartz was a later phase in the pegmatite and did not form until sapphirine was already isolated by Sil+Grt+Sur coronas However, the coronas are similar in mineral assemblage (except for the presence of Be minerals) to coronas in the host rocks, which suggests by analogy that sapphirine coexisted with quartz prior to formation of the coronas in the pegmatites None of the systems cited above contained Be, which preferentially enters sapphirine relative to the other solid phases except cordierite In contrast to the melted xenolith studied by Harley and Christy (1995), pressures for ultrahigh-temperature metamorphism of the Napier complex are estimated to have been 9–11 kbar, where cordierite has a limited stability field We think it more likely that in a Be-bearing system at pressures near 10 kbar, the sapphirine stability field could have had a sufficiently expanded so that Spr+Qtz became stable on the liquidus

These temperatures seem high for hornblende in the quartz-bearing pegmatite at Mt Charles However, F can stabilize amphiboles to higher temperatures relative to corresponding F-free amphiboles (nearly 100°C for pargasite with 0.86 F at 10 kbar under fluid absent conditions, Holloway and Ford, 1975), so that crystallization of the Mt Charles hornblende at ultrahigh temperatures cannot be ruled out, particularly in view of its high K_2O content

6.2. Isobaric cooling or polymetamorphism ?

Ellis (1980) was the first to propose that the peak-temperature conditions attained during ultrahigh-temperature metamorphism in the Napier Complex were followed by isobaric cooling, a conclusion accepted and further developed by most later workers (*e.g.*, Harley, 1983, 1985a, 1998a, Harley and Black, 1987, Sandiford, 1985a, Sheraton *et al.*, 1987) Harley (1985a) and Sandiford (1985a) attributed Opx+Sil coronas between sapphirine and quartz and "recrystallized trails" of fine-grained garnet similar texturally to the later-formed garnet in the Opx+Sil±Grt quartz granulites at Mt Pardoe to reactions during isobaric cooling in Khmara Bay and other areas south and west of Amundsen Bay Harley (1985a) did consider an alternative to continuous cooling from peak conditions, namely, that the reported conditions at each point on the P-T trajectory applied to a

discrete tectonothermal event He concluded that this alternative applied at least to the lower temperature part, *i.e*, M_3-D_3 at 600–750°C, but left open the question of a discrete event at higher temperatures between M_2-D_2 and M_3-D_3 Harley and Black (1987) did not mention the possibility of an event between M_2-D_2 and M_3-D_3, an interval of time during which the Napier Complex underwent cooling and then remained buried at depth

We suggest that the coronas in the pegmatites and host rocks are evidence for a discrete, high-temperature (>700°C) metamorphic event (Metamorphism-2, Table 13) following original crystallization and preceding M_3-D_3 Complete breakdown of sapphirine, together with strain that deformed the sillimanite—garnet—surinamite coronas into aggregates (in part foliated), requires more than simple cooling in a static environment The pegmatites must have been heated and stressed following crystallization, *i.e*, they were subjected to a metamorphic event, and are properly metapegmatites If the pegmatites were subjected to such an event, the host rocks must have been also, that is, the corona textures in the pegmatites and host rocks at "Christmas Point" were coeval and formed under the same *P-T* conditions The absence of orthopyroxene in the pegmatitic coronas could be due to its place being taken by surinamite in the Be-rich environment surrounding sapphirine-khmaralite Streaking of the fine-grained Sil+Opx aggregates in the host rocks implies these also were subjected to stress during recrystallization at high temperatures where the assemblage Sil+Opx+Qtz+Kfs/Fsp was stable

The corona texture is less obvious in the "Zircon Point" pegmatite, in which the beryllium-rich aggregates are surrounded by a margin of garnet (Grew, 1981) Grew (1998) cited parallel growth as evidence that khmaralite, musgravite, sillimanite and surinamite were coeval phases that formed during the second metamorphic event After study of samples collected in 1999 from "Christmas Point", the thin sections of the "Zircon Point" samples were reexamined Musgravite was found to embay khmaralite, and inclusions of khmaralite were found in garnet, musgravite and sillimanite These textures can be interpreted to mean that garnet, musgravite and sillimanite formed from breakdown of magmatic khmaralite (Table 13), a more plausible interpretation given the textural relations among these minerals in the "Christmas Point" pegmatites Textures in the Mt Pardoe pegmatites suggest a two-stage Late Archean evolution analogous to that inferred for "Christmas Point" (Table 13) An early generation of orthopyroxene and garnet appear to be pegmatitic, whereas sillimanite, surinamite and a second generation of orthopyroxene and garnet are metamorphic In the absence of evidence to the contrary, it seems most reasonable to suggest that the beryllian precursor to surinamite was sapphirine-khmaralite as is the case in the pegmatites at "Christmas" and "Zircon" Points In the Mt Charles pegmatite, hornblende reacted with quartz to form Opx+Pl coronas while lamellae of pyroxene developed within the hornblende itself

P-T conditions for the second metamorphic event at Mt Pardoe can be estimated in a very preliminary fashion from Aranovich and Berman (1996, Fig 7) using X_{Mg} of garnet and Al_2O_3 content of metamorphic orthopyroxene (Opx II) associated with sillimanite in sample no 10510B (Tables 10, 11) ~8–9 kbar, ~800°C This estimate could be too low, Al_2O_3 contents of 7 22–8 08 wt% in corona orthopyroxene in sample no 2282G from "Christmas Point" (0 307–0 341 Al/6O, X_{Mg}=0 723–0 720, Grew, unpublished data) suggest temperatures reached 900°C

Hensen and Motoyoshi (1992) presented evidence for a second ultrahigh-temperature

heating event at Mt Riiser-Larsen. Although not associated with penetrative deformation, Hensen and Motoyoshi's (1992) event could be equivalent to Metamorphism-2 proposed here.

6.3. Post-Archean metamorphism

Several minerals, notably andalusite, kyanite, cordierite and fine- to medium-grained biotite are attributed to two later metamorphic events that affected the beryllium pegmatites at all three localities (Metamorphism-3, -4, Table 13) These late-formed minerals are more abundant in the pegmatites than in the host rocks, most notably andalusite, which has only once been found in a non-pegmatitic rock (S Harley, personal communication, 2000, reports andalusite in a sheared and recrystallised gneiss from Tonagh Island). At "Christmas Point", the host rocks were extensively deformed and metamorphosed during the later two metamorphic events, so that kyanite and cordierite are abundant (Sandiford and Wilson, 1983, 1984; Sandiford, 1985b; Harley, 1985b), whereas at Mt. Pardoe, cordierite is rare and kyanite, absent, in the host rocks Most likely, microclinization of alkali feldspar occurred during this event, we infer that alkali feldspar originally crystallized with a relatively high degree of Al-Si disorder at the high temperatures inferred for pegmatite intrusion.

The presence of Al_2SiO_5 phases in close proximity to alkali feldspar implies low activities of water in parts of the pegmatites, whereas muscovite implies introduction of aqueous fluids in other parts The orthopyroxene selvages between cordierite and quartz could also have formed where water activities were low enough to stabilize a pyroxene instead of amphibole at relatively low temperatures, a situation reported in metapelitic rocks of the Strangways Range, Australia (Ballèvre *et al.*, 1997) The relatively low Al_2O_3 contents of this orthopyroxene, despite the proximity of Al-rich minerals such as cordierite and sillimanite, are indicative of temperatures below ~700°C (extrapolating from Aranovich and Berman, 1996, Fig. 7) Replacement of sillimanite by andalusite (Fig. 6a) is consistent with the decompression *P-T* path inferred for the late metamorphic events by Sandiford (1985b) and Harley (1985b), but the path should now be extended to $P<3$ kbar required by the presence of andalusite at ~600°C

7. Origin of the beryllium

Among the major questions posed by the beryllium pegmatites are the source of beryllium and the mechanisms for its transport and concentration Overall, Be minerals probably constitute less than 0.1% of the beryllium pegmatites, which would translate into a bulk Be content of a few ppm to a few tens ppm in the pegmatite, and thus the pegmatites are not particularly enriched relative to the host quartz-granulites Nonetheless, there must be some mechanism of Be concentration for any Be mineralization to appear in the pegmatites Most Late Archean pegmatites in the Napier Complex are barren, and, in general, beryllium enrichments are rare in pegmatites associated with granulite-facies rocks, the so-called abyssal class of pegmatites (*e.g.*, Černý, 1992) On the basis of available data, we suggest that the Late Archean pegmatites are most likely partial melts derived from the pelitic rocks hosting the pegmatites and that the beryllium originated from these host rocks

and was subsequently mobilized and concentrated in the melts

Several mineralogical and chemical features provide support for the assumption by Sandiford and Wilson (1984, 1986) and Black *et al* (1983) that the Late Archean pegmatites are locally derived anatectic melts Sandiford and Wilson (1986) cited geochemical evidence for local derivation of a "granulite-facies" pegmatite at "Zircon Point" whose trace element chemistry is similar to that of felsic gneisses in Khmara Bay Our data show an approximate correspondence between host rock major-element composition and pegmatite mineralogy as follows

1) The "Christmas Point" host rocks are more aluminous than the Mt Pardoe host rocks, *i.e*, average ASI index=mole Al/(K+Na+2Ca)=1·2±7 for "Christmas Point" *vs* 4·5±2 for Mt Pardoe (Tables 2 and 3) This is reflected in the presence of pegmatitic sillimanite but no pegmatitic orthopyroxene in the "Christmas Point" pegmatites, whereas the converse applies to the Mt Pardoe pegmatites
2) The k index (=mole K/(K+Na) is higher for the "Christmas Point" host rocks (k= 0·71±0·1) than for the Mt Pardoe host rocks (k=0·46±0·1) This is consistent with the dominance of microcline in the "Christmas Point" pegmatites, whereas a more sodic feldspar, mesoperthite, is dominant at Mt Pardoe
3) The host rocks at "Christmas Point" appear on the whole to be more oxidized than the host rocks at Mt Pardoe, and the "Christmas Point" pegmatites clearly are more so (see above)
4) Low Cr contents of the "Christmas Point" host rocks is reflected in negligible Cr contents in pegmatitic musgravite and spinel, minerals that are normally "sinks" for Cr
5) Zircon is a relatively abundant accessory mineral in several of the Late Archean pegmatites at "Zircon Point" (whence the name) and "Christmas Point", but the beryllium pegmatites at these localities contain little or no zircon That the relatively elevated Zr contents of the "Christmas Point" host rocks have not resulted in abundant zircon in all of the pegmatites at this locality could be due to slow dissolution of zircon in the host rock relative to melt extraction under dry conditions (Watt and Harley, 1993)

It could be argued that the effects on pegmatite mineral assemblage and chemistry attributed to differences in host rock ASI index, k index and degree of oxidation (no 1-3 above) resulted from interaction of the host rock with melt after intrusion However, if wall rock interaction were an important determinant of pegmatite mineral assemblages, one would expect the mineral assemblages in Early Paleozoic pegmatites to also reflect wall-rock compositions This is not the case (see below), and thus we think that it is justified to assume, pending further study, that source rock, rather than wall rock, has greater influence on the mineral assemblages and compositions of the Late Archean pegmatites

As regards the source of Be, possible mechanisms for its mobilization may play a more important role than its actual abundance in the host rocks The host rocks are not enriched in Be when compared either to the value calculated for the composition of the upper continental crust as a whole (3 ppm Be, Taylor and McLennan, 1995, Wedepohl, 1995), or to average Be contents of pelitic and semi-pelitic rocks in general, both unmetamorphosed and metamorphosed (1-4 ppm Be, *e.g*, Beus, 1966, Hörmann, 1969, Lebedev and Nagaytsev, 1980, Sheraton *et al*, 1984, Ryan and Langmuir, 1988, Ryan, 1989, Bushlyakov and Grigor'yev, 1989, Bebout *et al*, 1993) However, in contrast to the

pelitic rocks cited above, including the Prydz Bay granulites studied by Sheraton *et al* (1984), beryllium in "Christmas Point" and Mt Pardoe granulites appears to be largely fixed in sapphirine This mineral contains from two to three orders of magnitude more Be than the host rock In contrast, sillimanite is unlikely to contain a significant proportion of beryllium: in no 10501, it contains ≤ 2 ppm Be *vs* 227–249 ppm Be in associated sapphirine (Be contents of garnet and orthopyroxene have not been determined) Thus, sapphirine must have played a critical role in the transfer of beryllium from the host rocks to the anatectic melt The presence of the relatively F-rich minerals in the pegmatites, wagnerite, ideally $(Mg,Fe)_2PO_4F$, and biotite, suggests a possible role for fluorine in this transfer, and fluorine enrichment of fluids at high temperatures is consistent with the thermodynamic analysis of Zhu and Sverjensky (1991) Whether fluorine can mobilize beryllium at ultrahigh temperatures is not known, but in its absence, beryllium is considered to be a relatively immobile element (Ryan, 1989, Ryan and Langmuir, 1988) Wood (1992) calculated that fluoride complexes could mobilize Be at low temperatures, whereas qualitative experiments provide evidence for mobilization at moderate temperatures (490–540°C, Beus *et al* , 1963)

The Late Archean pegmatites can be contrasted to the generation of early Paleozoic pegmatites, which also contain beryllium minerals, most often beryl, or, less commonly, chrysoberyl, as well as the rare-element minerals tourmaline, dumortierite and columbite-tantalite (Grew, 1981, Sandiford, 1985b). However, the presence of primary muscovite indicates intrusion at temperatures well below those inferred for the Late Archean pegmatites In general, the mineral assemblages of the early Paleozoic pegmatites show less correspondence with host rock composition compared to the Late Archean pegmatite, implying a smaller contribution from locally derived material. Isotopic data show evidence for an Archean signature from the host rocks in the high $^{207}Pb/^{204}Pb = 16\,32$ of one early Proterozoic pegmatite (Grew and Manton, 1979), but no host-rock signature was evident in the initial $^{87}Sr/^{86}Sr$ ratio of another pegmatite of this generation (Black *et al* , 1983). Compared to the Late Archean pegmatites, the aureoles associated with the early Paleozoic pegmatites are volumetrically much more extensive and have retrograded the country rock Evidently, the early Paleozoic pegmatites must have been associated with considerable aqueous fluid, which could have introduced boron and other rare elements from a distant source We agree with Sandiford (1985b) that B in the early Paleozoic pegmatites could not have originated in the Napier Complex Granulite-facies rocks are characterized by extreme depletion in B (*e.g* , Leeman and Sisson, 1996) and the Napier Complex appears to be no exception As far as we are aware, the only report of B-bearing minerals in Napier Complex granulite-facies rocks is the "Zircon Point" beryllium pegmatite, *e.g* , dumortierite (see above) Most likely, as suggested by Sandiford (1985b), the source of Be, as well as B, for the early Paleozoic pegmatites was outside the Napier Complex even though Be, unlike B, was available in Napier complex rocks

8. Conclusion

On the basis of samples collected on JARE-40 in January, 1999, a new scenario is proposed for the origin of beryllium pegmatites, four of which have been found at three localities in the Napier Complex Evolution of the pegmatites can be divided into three

major stages (Table 13) The first stage involves partial melting of sapphirine-bearing metapelites soon after peak temperatures were attained during ultrahigh-temperature metamorphism and crystallization of the melts as pegmatites in inter-boudin spaces during the waning stages of deformation associated with this metamorphism, *i.e* , the Late Archean M_1-D_2 event of Sandiford and Wilson (1983, 1984) A possible source of Be was sapphirine in quartz-rich granulites that presently host the pegmatites The primary carrier of beryllium in the pegmatites at the time of their intrusion was a sapphirine-group mineral Other minerals inferred to have crystallized from the melt include quartz, K-feldspar (which subsequently inverted to microcline), sillimanite, wagnerite and Ti-bearing biotite at "Christmas Point", orthopyroxene, instead of sillimanite, was probably a primary phase at Mt Pardoe The mineral assemblages suggest very low water activities and high temperatures (probably >900°C) during melting and crystallization of the pegmatites

The second stage is high-temperature metamorphism, which resulted in reaction of sapphirine with quartz to form corona assemblages of Sil+Opx (or Grt) in the host rocks and Sil+Grt+Sur in the beryllium pegmatites Sil+Grt+Sur aggregates in the pegmatites formed when beryllian sapphirine-khmaralite completely reacted away and the coronas were deformed beyond recognition Previous investigators have attributed the corona assemblages in the host rocks to isobaric cooling following ultrahigh-temperature metamorphism (*e.g* , Harley and Black, 1987) However, the relatively large size of the coronas and their deformation in the pegmatites suggests that the coronas formed during a separate tectonothermal event, which affected host rock and pegmatites alike Water activities remained low The age of metamorphism is unknown

The third stage includes two metamorphic events at lower temperatures and moderate to low pressures when all three Al_2SiO_5 phases and abundant Ti-poor biotite formed in the pegmatite The only third-stage mineral found to contain significant beryllium is cordierite formed by breakdown of surinamite Water activities varied so that Al_2SiO_5+ K-feldspar or Al-poor orthopyroxene was stable in some parts of the pegmatite, whereas muscovite, chlorite or orthoamphibole formed in others These metamorphic events have not been dated precisely, but ages between 1100 and 500 Ma seem most likely, early Paleozoic pegmatites that are associated with metamorphic aureoles have been dated at 520 Ma (Black *et al* , 1983)

Given the presence of the fluorphosphate wagnerite and the relatively high F and Cl contents of both early and late biotite, clearly F and Cl played an important role throughout the evolution of the pegmatite The exact nature of this role needs further study, as do the conditions under which sapphirine crystallizes in peraluminous granitic melts Another question concerns the geochemical role of beryllium Although Be is present in Napier Complex metapelitic rocks in amounts averaging only 3–4 ppm, partial melting of these rocks at very high-temperatures and very low water activities has sufficiently concentrated Be for Be-bearing minerals to form in pegmatite crystallizing from these melts

Acknowledgments

We thank the crews of the two helicopters based at Tonagh Island camp (Messrs Y Ohashi, K Maki, S Harigai, T Takei), Dr H Yamauchi, and Dr Y Yoshimura for

logistical support at Mt Pardoe and Tonagh Island Special thanks goes to the Captain and crew of the icebreaker "Shirase" for arranging and carrying out a special helicopter flight to "Christmas Point" on January 22, 1999, without which this study would not have been possible The constructive reviews of an earlier draft by Simon Harley, Bas Hensen, and Yoshikuni Hiroi improved the paper considerably, for which we are grateful We also thank Thomas Armbruster and Clivia Hejny for information on the polysome of högbomite in no. 12227, Chris Carson for a specimen of quartz granulite from Mt Pardoe, Chris Carson and Dan Dunkley for information on the GPS readings, Dan Dunkley for photographs of one "Christmas Point" beryllium pegmatite, D Hudson for a specimen of Musgrave Ranges beryllian sapphirine (no 14820; Wilson and Hudson, 1967) K. Kitamura for assistance in preparing the photographs and Ulrich Senff for assistance with the whole-rock chemical analysis. ESG's and MGY's research was supported by U S National Science Foundation grant OPP-9813569 to the University of Maine The SIMS analyses were performed at the NSF-sponsored University of New Mexico (UNM)/Sandia National Laboratories (SNL) ion microprobe facility, a joint operation of the UNM Institute of Meteoritics and SNL

References

Aranovich, L Ya and Berman, R G (1996) Optimized standard state and solution properties of minerals II Comparisons, predictions, and applications Contrib Mineral Petrol, **126**, 25-37

Baba, S, Grew, E S, Shearer, C K and Sheraton, J W (1999) Surinamite, a high-temperature metamorphic beryllosilicate, from Lewisian kyanite+orthopyroxene+quartz+alkali feldspar gneiss at South Harris, Scotland Geol Soc Am Abstracts with Programs, **31**(7), A-306

Baba, S, Grew, E S, Shearer, C K and Sheraton, J W (2000) Surinamite, a high-temperature metamorphic beryllosilicate, from Lewisian sapphirine-bearing kyanite+orthopyroxene+quartz+K-feldspar gneiss at South Harris, NW Scotland Am Mineral (in press)

Ballèvre, M, Hebsen, B J and Reynard, B (1997) Orthopyoxene-andalusite symplectites replacing cordierite in granulites from the Strangways Range (Arunta block, central Australia) A new twist to the pressure-temperature history Geology, **25**, 215-218

Barbier, J, Grew, E S, Moore, P B and Su, S-C (1999) Khmaralite, a new beryllium-bearing mineral related to sapphirine A superstructure resulting from partial ordering of Be, Al and Si on tetrahedral sites Am Mineral, **84**, 1650-1660

Bebout, G E, Ryan, J G and Leeman, W P (1993) B-Be systematics in subduction-related metamorphic rocks Characterization of the subducted component Geochim Cosmochim Acta, **57**, 2227-2237

Beus, A A (1966) Geochemistry of Beryllium and Genetic Types of Beryllium Deposits San Francisco, Freeman, 401 p

Beus, A A, Sobolev, B P and Dikov, Yu P (1963) Geochemistry of beryllium in high temperature postmagmatic mineralization Geochemistry, **1963**, 316-323

Black, L P, James, P R and Harley, S L (1983) Geochronology and geological evolution of metamorphic rocks in the Field Islands area, East Antarctica J Metamorph Geol, **1**, 277-303

Bushlyakov, I N and Grigor'yev, N A (1989) Beryllium in Ural metamorphites Geochem Internat, **26**(4), 57-61

Černý, P (1992) Geochemical and petrogenetic features of mineralization in rare-element granitic pegmatites in the light of current research Appl Geochem, **7**, 393-416

Christy, A G (1988) A new 2*c* superstructure in beryllian sapphirine from Casey Bay, Enderby Land, Antarctica Am Mineral, **73**, 1134-1137

Christy, A G (1989) The effect of composition, temperature and pressure on the stability of the 1Tc and 2M polytypes of sapphirine Contrib Mineral Petrol, **103**, 203–215

Deer, W A, Howie, R A and Zussman, J (1997) Rock-Forming Minerals, vol 2B, Double-chain Silicates, 2nd ed London, The Geological Society, 764 p

De Roever, E W F and Vrána, S (1985) Surinamite in pseudomorphs after cordierite in polymetamorphic granulites from Zambia Am Mineral, **70**, 710–713

Ellis, D J (1980) Osumilite-sapphirine-quartz granulites from Enderby Land, Antarctica *P-T* conditions of metamorphism, implications for garnet-cordierite equilibria and the evolution of the deep crust Contrib Mineral Petrol, **74**, 201–210

Foster, W R (1950) Synthetic sapphirine and its stability relations in the system MgO-Al_2O_3-SiO_2 J Geol, **58**, 135–151

Franz, G and Morteani, G (1984) The formation of chrysoberyl in metamorphosed pegmatites J Petrol, **25**, 27–52

Gatehouse, B M and Grey, I E (1982) The crystal structure of hogbomite-8H Am Mineral, **67**, 373–380

Grew, E S (1980) Sapphirine+quartz association from Archean rocks in Enderby Land, Antarctica Am Mineral, **65**, 821–836

Grew, E S (1981) Surinamite, taaffeite, and beryllian sapphirine from pegmatites in granulite-facies rocks of Casey Bay, Enderby Land, Antarctica Am Mineral, **66**, 1022–1033

Grew, E S (1998) Boron and beryllium minerals in granulite-facies pegmatites and implications of beryllium pegmatites for the origin and evolution of the Archean Napier Complex of East Antarctica Mem Natl Inst Polar Res, Spec Issue, **53**, 74–92

Grew, E S and Manton, W I (1979) Archean rocks in Antarctica 2 5 billion-year uranium-lead ages of pegmatites in Enderby Land Science, **206**, 443–445

Grew, E S, Manton, W I and Sandiford, M (1982) Geochronologic studies in East Antarctica Age of pegmatites in Casey Bay, Enderby Land Antarct J U S, **17**(5), 1–2

Grew, E S, Chernosky, J V, Werding, G, Abraham, K, Marquez, N and Hinthorne, J R (1990) Chemistry of kornerupine and associated minerals, a wet chemical, ion microprobe, and X-ray study emphasizing Li, Be, B and F contents J Petrol, **31**, 1025–1070

Grew, E S, Redhammer, G J, Amthauer, G, Cooper, M A, Hawthorne, F C and Schmetzter, K (1999) Iron in kornerupine A ^{57}Fe Mossbauer spectroscopic study and comparison with single-crystal refinement Am Mineral, **84**, 536–549

Harley, S (1983) Regional geobarometry-geothermometry and metamorphic evolution of Enderby Land, Antarctica Antarctic Earth Science, ed by R L Oliver *et al* Canberra, Aust Acad Science, 25–30

Harley, S (1985a) Garnet-orthopyroxene bearing granulites from Enderby Land, Antarctica Metamorphic pressure-temperature-time evolution of the Archaean Napier Complex J Petrol, **26**, 819–856

Harley, S (1985b) Paragenetic and mineral-chemical relationships in orthoamphibole-bearing gneisses from Enderby Land, east Antarctica a record of Proterozoic uplift J Metamorph Geol, **3**, 179–200

Harley, S L (1998a) On the occurrence and characterization of ultrahigh-temperature crustal metamorphism What Drives Metamorphism and Metamorphic reactions?, ed by P J Treloar and P J O'Brien London, Geol Soc, 81–107 (Spec Publ 138)

Harley, S L (1998b) An appraisal of peak temperatures and thermal histories in ultrahigh-temperature (UHT) crustal metamorphism the significance of aluminous orthopyroxene Mem Natl Inst Polar Res, Spec Issue, **53**, 49–73

Harley, S L and Black, L P (1987) The Archaean geological evolution of Enderby Land, Antarctica Evolution of the Lewisian and Comparable Precambrian High Grade Terrains, ed by R G Park and J Tarney London, Geol Soc, 285–296 (Spec Publ 27)

Harley, S L and Black, L P (1997) A revised Archaean chronology for the Napier Complex, Enderby Land, from SHRIMP ion-microprobe studies Antarct Sci, **9**, 74–91

Harley, S L and Christy, A G (1995) Titanium-bearing sapphirine in a partially melted aluminous granulite xenolith, Vestfold Hills, Antarctica geological and mineralogical implications Eur J Mineral, **7**, 637–653

Hensen, B J and Motoyoshi, Y (1992) Osumilite-producing reactions in high temperature granulites from the Napier Complex, East Antarctica tectonic implications Recent Progress in Antarctic Earth Science, ed by Y Yoshida *et al* Tokyo, Terra Sci Publ, 87–92

Holloway, J R and Ford, C E (1975) Fluid-absent melting of the fluoro-hydroxy amphibole pargasite to 35 kilobars Earth Planet Sci Lett, **25**, 44–48

Hormann, P K (1969) Handbook of Geochemistry, Beryllium B-O Berlin, Springer

Keith, M L and Schairer, J F (1952) The stability field of sapphirine in the system MgO-Al_2O_3-SiO_2 J Geol, **60**, 181–186

Kretz, R (1983) Symbols for rock-forming minerals Am Mineral, **68**, 277–279.

Leake, B E (1968) A catalog of analyzed calciferous and subcalciferous amphiboles together with their nomenclature and associated minerals Geol Soc Am Spec Paper, **98**, 1–210

Lebedev, V I and Nagaytsev, Yu V (1980) Minor elements in metamorphic rocks as an ore-material source for certain deposits Geochem Internat, **17**(6), 31–39

Leeman, W P and Sisson, V B (1996) Geochemistry of boron and its implications for crustal and mantle processes Boron Mineralogy, Petrology and Geochemistry, ed by E S Grew and L M Anovitz Washington, D C, Mineral Soc Am, 645–707 (Rev Mineral, vol 33)

Liu, T-C and Presnall, D C (1990) Liquidus phase relations on the join anorthite-forsterite-quartz at 20 kbar with applications to basalt petrogenesis and igneous sapphirine Contrib Mineral Petrol, **104**, 735–742

Liu, T-C and Presnall, D C (2000) Liquidus phase relations in the system CaO-MgO-Al_2O_3-SiO_2 at 2 0 GPa applications to basalt fractionation, eclogites, and igneous sapphirine J Petrol, **41**, 3–20

Milholland, C S and Presnall, D C (1998) Liquidus phase relations in the CaO-MgO-Al_2O_3-SiO_2 system at 3 0 GPa the aluminous pyroxene thermal divide and high-pressure fractionation of picritic and komatiitic magmas J Petrol, **39**, 3–27

Moore, P B and Araki, T (1983) Surinamite, *ca* $Mg_3Al_4Si_3BeO_{16}$ Its crystal structure and relation to sapphirine, *ca* $Mg_{2\,8}Al_{7\,2}Si_{1\,2}O_{16}$ Am Mineral, **68**, 804–810

Motoyoshi, Y and Hensen, B J (1989) Sapphirine-quartz-orthopyroxene symplectites after cordierite in the Archaean Napier Complex, Antarctica evidence for a counterclockwise *P-T* path ? Eur J Mineral, **1**, 467–471

Petersen, E U, Essene, E J, Peacor, D R and Valley, J W (1982) Fluorine end-member micas and amphiboles Am Mineral, **67**, 538–544

Petersen, E U, Essene, E J, Peacor, D R and Marcotty, L A (1989) The occurrence of hogbomite in high-grade metamorphic rocks Contrib Mineral Petrol, **101**, 350–360

Ryan, J G (1989) The systematics of lithium, beryllium and boron in young volcanic rocks Ph D thesis, Columbia University, 310 p

Ryan, J G and Langmuir, C H (1988) Beryllium systematics in young volcanic rocks implications for ^{10}Be Geochim Cosmochim Acta, **52**, 237–244

Sahama, T G, Lehtinen, M and Rehtijarvi, P (1974) Properties of sapphirine Ann Acad Sci Fenn, Ser A, III Geol-Geogr, **114**, 1–24

Sandiford, M (1985a) The metamorphic evolution of granulites at Fyfe Hills, implications for Archaean crustal thickness in Enderby Land, Antarctica J Metamorph Geol, **3**, 155–178

Sandiford, M (1985b) The origin of retrograde shear zones in the Napier Complex implications for the tectonic evolution of Enderby Land, Antarctica J Struct Geol, **7**, 477–488

Sandiford, M and Powell, R (1986) Pyroxene exsolution in granulites from Fyfe Hills, Enderby Land, Antarctica Evidence for 1000°C metamorphic temperatures in Archean continental crust Am Mineral, **71**, 946–954

Sandiford, M and Wilson, C J L (1983) The geology of the Fyfe Hills-Khmara Bay region, Enderby Land Antarctic Earth Science, ed by R L Oliver *et al* Canberra, Aust Acad Sci, 16–19

Sandiford, M and Wilson, C J L (1984) The structural evolution of the Fyfe Hills-Khmara Bay region, Enderby Land, East Antarctica Aust J Earth Sci , **31**, 403-426

Sandiford, M and Wilson, C J L (1986) The origin of Archaean gneisses in the Fyfe Hills region, Enderby Land, field occurrence, petrography and geochemistry Precambrian Res , **31**, 37-68

Schmetzer, K (1983) Crystal chemistry of natural Be-Mg-Al-oxides taaffeite, taprobanite, musgravite Neues Jahrb Mineral Abh , **146**, 15-28

Sheraton, J W (1980) Geochemistry of Precambrian metapelites from East Antarctica secular and metamorphic variations BMR J Aust Geol Geophys , **5**, 279-288

Sheraton, J W (1985) Chemical analyses of rocks from East Antarctica Part 2 Australia Bureau of Mineral Resources, Geology and Geophysics Record 1985/12, 124 p

Sheraton, J W , Black, L P and McCulloch, M T (1984) Regional geochemical and isotopic characteristics of high-grade metamorphics of the Prydz Bay area the extent of Proterozoic reworking of Archaean continental crust in East Antarctica Precambrian Res , **26**, 169-198

Sheraton, J W , Tingey, R J , Black, L P, Offe, L A and Ellis, D J (1987) Geology of an unusual Precambrian high-grade metamorphic terrane-Enderby Land and western Kemp Land, Antarctica BMR Bull , **223**, 51 p

Taylor, S R and McLennan, S M (1995) The geochemical evolution of the continental crust Rev Geophys , **33**, 241-265

Watt, G R and Harley, S L (1993) Accessory phase controls on the geochemistry of crustal melts and restites produced during water-undersaturated partial melting Contrib Mineral Petrol , **114**, 550-566

Wedepohl, K H (1995) The composition of the continental crust Geochim Cosmochim Acta, **59**, 1217-1232

Wilson, A F and Hudson, D R (1967) The discovery of beryllium-bearing sapphirine in the granulites of Musgrave Ranges (Central Australia) Chem Geol , **2**, 209-215

Wood, S A (1992) Theoretical prediction of speciation and solubility of beryllium in hydrothermal solution to 300°C at saturated vapor pressure Application to bertrandite/phenakite deposits Ore Geol Rev , **7**, 249-278

Zhu, C and Sverjensky, D A (1991) Partitioning of F-Cl-OH between minerals and hydrothermal fluids Geochim Cosmochim Acta, **55**, 1837-1858

(Received February 22, 2000, Revised manuscript accepted April 14, 2000)